Functional analysis of L-type amino acid transporter 3 (*LAT3*) in prostate cancer: the relationship with androgen receptor and downstream target

（前立腺癌におけるアミノ酸トランスポーターLAT3 の機能解析）

千葉大学大学院医学薬学府

先端医学薬学専攻

（主任：市川智彦教授）

梨井　隼菱

Introduction

Prostate cancer (PC) is the second most common cancer among men worldwide[1]. The androgen receptor (AR) is crucial for not only the normal growth and maintenance of the prostate gland, but also the development of PC[2]. Androgen deprivation therapy is regarded as the standard treatment for metastatic PC, and although it may show effectiveness initially, PC often develops resistance to the therapy and progresses to fatal castration-resistant prostate cancer (CRPC)[3-8]. Several schemes for the transition to CRPC have been postulated, and AR plays a central role in them[9-12]. Cancer cells require large amounts of amino acids for their survival, and their uptake into the cell is facilitated by amino acid transporters[13, 14]. L-type amino acid transporter 3 (LAT3, *SLC43A1*) takes neutral amino acids, including leucine, isoleucine, valine, phenylalanine, and methionine, into cells[15]. LAT3 was originally identified as a gene *(POV1)* that was overexpressed in PC[16] and subsequently revealed to be an amino acid transporter[17]. Therefore, it may be possible that LAT3 plays an important role in PC growth through amino acid uptake. A recent study revealed that in PC, LAT3 coordinates mammalian target of rapamycin complex 1 (mTORC1), which requires intracellular leucine for its activation[18]. However, the function of LAT3 in the AR pathway and its downstream target gene are not well documented. In this study, we attempted to elucidate the function of LAT3 in AR pathway and its downstream target gene. We also retrospectively investigated the LAT3 expression profile and its association with clinical parameters in PC specimens.

Materials and Methods

Cell Culture and Transfection

The human PC cell line LNCaP, PC3, and DU145 were obtained from the Cell Resource Centre for Biomedical Research, Institute of Development, Aging and Cancer, Tohoku University (Miyagi, Japan) and C4-2 was obtained from the American Type Culture Collection (Manassas, VA). Cell cultures were prepared in RPMI-1640 medium (FUJIFILM Wako, Osaka, Japan) supplemented with 10% foetal bovine serum (FBS) and penicillin-streptomycin solution (FUJIFILM Wako). These cells were maintained in a humidified atmosphere of 95% air and 5% CO_2 at 37°C. For steroid-free conditions, phenol red-free RPMI-1640 medium was used with 10% charcoal-stripped FBS (CSS). Mycoplasma contamination was tested using the CycleavePCR mycoplasma Detection kit (Takara Bio, Shiga, Japan) to confirm that the cultures were mycoplasma-free. Cells were transfected with small interfering RNA (siRNA) using Lipofectamine™ RNAiMAX (Thermo Fisher Scientific, Waltham, MA) according to the manufacturer's instructions and cells were harvested 72 hr after transfection.

Reagents and antibodies

In this study, Lipofectamine™ RNAiMax Transfection Reagent, OPTI-MEM, siRNAs SiLAT3 (Stealth siRNAs: HSS112400 and HSS189324), SiAR (HSS100619 and HSS179972) and Stealth RNAi siRNA Negative Control Med GC Duplex #3 were obtained from Thermo Fisher Scientific (Waltham, MA). pIRESpuro-mSeparase-WT-6myc was kindly provided by Dr. Toru Hirota and pcDNA3.1(+)-LAT3 was a kind gift provided by Dr. Naohiko Anzai. Anti-LAT3 (HPA018826) was obtained from Sigma (St. Louis, MO). Anti-AR (AR441, ab9474) was obtained from Abcam (Cambridge, MA). Anti-LAT1 (KE023) was obtained from Trans Genic Inc (Kobe, Japan). Anti-AKT, anti-phosphorylated AKT (Ser473), anti-

phosphorylated 4EBP-1, and anti-phosphorylated p70s6k (Thr389, Ser371), anti-phosphorylated mTOR (Ser2448), anti-mTOR, anti-E-cadherin, anti-N-cadherin, anti-Vimentin, anti-Slug were obtained from Cell Signalling Technology Inc. (Danvers, MA). Anti-glyceraldehyde 3-phosphate dehydrogenase (GAPDH) was obtained from Ambion Inc. (Carlsbad, CA). Dihydrotestosterone (DHT), bicalutamide, and MDV3100 were purchased from Sigma. Anti-Separase (WH0009700M1) was also obtained from Sigma and the Separse-specific inhibitor Sepin-1 was obtained from AOBIOUS Inc. (Gloucester, MA). Mitomycin C solution was obtained from Nacalai tesque (Kyoto, Japan).

Reverse transcription polymerase chain reaction (RT-PCR)

Total RNA was isolated using the RNeasy Mini Kit (Qiagen, Hilden, German) according to the manufacturer's instructions. RT-PCR was performed according to a protocol reported previously[19]. The *GAPDH* mRNA level was quantified for normalization control. The PCR primers used in this study are listed in Table S1.

Western blotting

Protein extraction and western blotting were performed as described previously[14]. The protein content was quantified using the bicinchoninic acid protein assay kit (Thermo Fisher Scientific), and protein samples (20 mg) were subjected to sodium dodecyl sulfate polyacrylamide gel electrophoresis (SDS-PAGE) using a gel prepared from the TGX Fastcast Acrylamide kit (10%, Bio-Rad, Hercules, CA) according to manufacturer's protocol. Block Ace (KAC co., Ltd, Kyoto, Japan) was used for membrane blocking. Band signals were detected by the luminescent Image Analyzer LAS-4000 mini (Fujifilm, Tokyo, Japan). The original full images of membranes are shown in Fig. S1 to S3.

Chromatin Immunoprecipitation (ChIP) assay and ChIP sequencing (ChIP-seq) analysis

In this study, we utilized our previously deposited NGS date GSE122922 (GSM3488490 – GSM3488508)[10] in Gene Expression Omnibus.

Cell viability assay

Cells were seeded into 96-well plates (3000 cells/well), and viability was determined using Cell Counting Kit-8 (CCK8; Dojindo, Kumamoto, Japan). At each time point, cells were incubated with CCK8 for 2 hr, and the absorbance was measured using Microplate Manager v6.0 (Bio-Rad). For assessing the Sepin-1 inhibitory effect, 24 hr after seeding, the medium was changed to medium containing Sepin-1 (for each concentration) or dimethyl sulfoxide (0.5%; vehicle control). The IC_{50}, which is defined as the drug concentration at which cell viability is reduced by half, was determined by GraphPad Prism 7 (GraphPad Software, La Jolla, CA) as described previously[20]. Three sets of independent experiments were performed for each time point.

Cell Migration and Invasion Assay

Falcon Cell Culture Insert (Corning Inc., Canton, NY) was used for the migration assay, and Biocoat Matrigel invasion chamber (Corning Inc.) was used for the invasion assay. The essential parts of the experiments have been described previously[14]. Briefly, 5000 cells were seeded into the upper chamber and incubated for 48 hr with serum-free medium. Cells were stained using Diff-Quik (Funakoshi, Tokyo, Japan). The cell numbers in five different fields at 100× magnification were determined under a microscope. Wound healing assay was performed as described previously[21].

RNA-seq analysis

Total RNA was isolated from LNCaP cells using the RNeasy Mini Kit (Qiagen). The detailed RNA-seq methods have been reported previously[10]. TopHat (v2.0.1) (https://ccb.jhu.edu/software/tophat/index.shtml) was used to align sequenced reads, and gene expression levels were quantified using Cufflinks (v2.2.1) (http://cole-trapnell-lab.github.io/cufflinks/). Gene ontology analysis was conducted using Metascape (https://metascape.org/gp/index.html#/main/step1)[22].

Flow cytometric analysis

Cell cycle analysis was performed using an HS800 cell sorter (Sony, Tokyo, Japan) as described previously[10]. LNCaP cells were transfected with SiLAT3 for 72 hr, then analysed.

Analysis of clinical PC patient datasets

Two cohort datasets of clinical PC patient information were analysed in this study. Datasets from Grasso et al (GSE35988)[23] and Luo et al[24] were obtained through Oncomine (https://www.oncomine.org/resource/main.html).

PC Tissue Specimens

PC tissue specimens and clinical information were obtained from 95 patients who received radical prostatectomy at Chiba University Hospital (Chiba, Japan) between 2006 and 2011. Histopathological assessment of the tissues was conducted according to the World Health Organization classification of PC by the Department of Pathology, Chiba University Hospital. The clinical and pathological stages were determined according to the TNM classification of the

International Union Against Cancer. The patient data are summarized in Table 2.

Ethical approval and consent to participate

The present study was carried out in accordance with the Declaration of Helsinki and ethical standards that promote and ensure respect and integrity for all human subjects. The institutional review board of Chiba University Hospital approved this study (approval no. 914), and all patients provided written informed consent for participation before surgery.

Immunohistochemistry (IHC)

The detailed IHC methods have been reported previously [25]. Anti-LAT3 antibody (1:200 dilution), anti-Separase antibody (1:100 dilution), anti-LAT1 antibody (1:100 dilution), and anti p-4EBP1 (1:400 dilution) were used. To quantify LAT3, LAT1, and Separase protein expression in these components, we applied the previously described IHC scoring method[19]. LAT3, LAT1, and Separase IHC scores over the median scores were defined as positive. For immunostaining of p4EBP1, 10 cases were randomly selected from the LAT3 High and Low groups and stained for scoring. The expression levels were scored by two independent investigators (AF and JR) who were blinded to patient clinical and pathological information.

Statistical analysis

Univariate and multivariate Cox proportional models were used to analyse statistical associations between clinical factors, pathological factors, IHC scores, and recurrence-free survival (RFS). RFS was defined as the period from prostatectomy to prostate-specific antigen recurrence. Survival curves were obtained using the Kaplan-Meier method, and differences in survival rates were compared using the log-rank test. The Wilcoxon signed-rank test and chi-square test were

used to assess associations between the LAT3 or Separase IHC score and clinical factors. The unpaired Student's t-test was used for assessing differences between two groups. Statistical analyses were performed using JMP Pro version 13.0.0 (SAS Institute, Cary, NC). Statistical significance was set at P values below 0.05.

Results

LAT3 expression and relationship with AR in PC cell lines and clinical PC datasets

First, we evaluated the expression of LAT3 in several PC cell lines. LAT3 was abundantly expressed in LNCaP and C4-2 cells that express AR, but it was hardly expressed in PC3 and DU145 cells that do not express AR (Fig. 1A, B). In the publicly available clinical PC datasets, the *LAT3* mRNA levels were significantly elevated in PC tumours when compared to the normal controls, but there was no significant difference between CRPC and localized cancer (Fig. S4A, B). In addition, LAT3 expression was also significantly increased in cases with amplified AR (Fig. S4C). When cultured in CSS medium, there was little or no LAT3 expression in either cell line (Fig. 1A, B). When LNCaP and C4-2 cells were cultured in CSS medium, stimulation by DHT (0.1 nM, 1 nM, or 10 nM) increased LAT3 expression in a dose-dependent manner (Fig. 1C, D). The effect of DHT on LAT3 expression was suppressed by bicalutamide (10 μM; Fig. 1C, D). Similarly, AR expression was also reduced in CSS medium, but markedly increased by DHT administration, and this effect was suppressed by bicalutamide (Fig. 1E, F).

Effects of AR knockdown on LAT3 expression and LAT3 knockdown on the mTOR pathway

To further investigate the relationship between AR and LAT3, we performed an AR

knockdown experiment using siRNA. AR knockdown significantly reduced LAT3 expression in LNCaP (Fig. 2A, B) and C4-2 (Fig. 2C, D) cells. Similarly, when the medium was changed to CSS for LNCaP cells, the expression of LAT3 decreased in a time-dependent manner (Fig. 2E). In ChIP-seq of AR, the genome browser view showed binding of AR at the LAT3 locus in DHT-stimulated LNCaP cells (Fig. 2F). To further investigate the regulation of LAT3 expression by AR, we performed motif analysis of the AR binding site in LAT3 and identified the AR-halfsite motif. (Figure S5). Next, we confirmed that SiLAT3 significantly reduced LAT3 expression (Fig. 2G, H). Furthermore, LAT3 knockdown inhibited the phosphorylation of the mTOR, eukaryotic translation initiation factor 4EBP1, and ribosomal protein S6K1, but not the phosphorylation of Akt (Fig. 2I). AR knockdown showed similar results (Fig. S6).

Inhibition of cell growth, migration, and invasion by LAT3 knockdown and rescue study of LAT3

We assessed the effect of LAT3 knockdown on the proliferation activities of PC cells. In LNCaP cells, LAT3 knockdown significantly suppressed the cell growth (Fig. 3A), migration activity (Fig. 3B), and invasion activity (Fig. 3C) of the cells when compared to the negative control. In C4-2 cells under the castrated condition (in CSS medium), LAT3 knockdown did not decrease the cell growth (Fig. 3D), migration activity (Fig. 3E), or invasion activity (Fig. 3F) of the cells. In contrast, when C4-2 cells were cultured under normal conditions (in FBS), LAT3 knockdown significantly inhibited the cell growth (Fig. 3G), migration activity (Fig. 3H), and invasion activity (Fig. 3I) of the cells when compared to the negative control. Furthermore, wound healing assay was performed, and the same results were obtained by LAT3 knockdown. (Fig. S7A, B, C). We next investigated the expression changes of EMT-related proteins (eg, E-Cadherin, N-Cadherin, Slug, Vimentin) by LAT3 knockdown (Fig. S7D). Notably, the expression level of E-Cadherin was upregulated, and N-Cadherin, Slug, and Vimentin were

suppressed by SiLAT3 (Fig. S7D). In addition, under the condition that the expression of LAT3 was suppressed by MDV3100, an anti-androgenic drug, introduction of LAT3 significantly restored cell proliferation compared to cells transfected with control vector (Figure S8A). We confirmed that LAT3 transfection restored LAT3 protein expression in MDV3100 treated cells (Figure S8B). Collectively, these results indicated that LAT3 knockdown has inhibitory effects on cell growth, migration, and invasion in an androgen-dependent manner.

Identification of LAT3 downstream target genes

To further elucidate the functional mechanism of LAT3 in PC, we extracted candidate LAT3 target genes by RNA-Seq analysis of LNCaP cells treated with SiLAT3. The genes downregulated by SiLAT3 were significantly associated with gene ontology terms such as "cell cycle", "DNA replication", and "cell division" (Fig. 4A). The top 10 genes that were downregulated by SiLAT3 are listed in Fig. 4B. These genes were confirmed by RT-PCR (Fig. 4C). Based on the basal expression levels and reproducibility, we selected Separase (*ESPL1*), which is known to play an important role in the cell cycle of cancer cells[26, 27]. First, we confirmed that the expression of Separase was reduced by LAT3 knockdown (Fig. 4D). In the cell cycle analysis, LAT3 knockdown significantly decreased the number of cells in the S and G2/M phases, suggesting cell cycle arrest (Fig. 4E). We then tested the effect of Sepin-1, a selective Separase inhibitor[28], on PC cell growth. The IC_{50} of Sepin-1 in LNCaP cells was 5.99 μM (Fig. 4F). Sepin-1 inhibited the proliferation of LNCaP cells in a dose-dependent manner (Fig. 4G). Combined treatment with Sepin-1 and MDV3100~~, an anti-androgenic drug,~~ inhibited cell proliferation in an additive manner (Fig. 4H). To confirm the additive effect of Sepin-1 and anti-androgenic drug, proliferation studies were conducted using Sepin-1 and apalutamide, another anti-androgenic drug, which also inhibited cell proliferation in an additive manner

(Fig.S9A). Moreover, when cultured in CSS medium, Sepin-1 showed an inhibitory effect on proliferation of LNCaP cells (Fig.S9B). In addition, introduction of both Separase and SiLAT3 significantly restored cell proliferation compared to cells transfected with SiLAT3 alone (Figure S8C). We confirmed that Separase transfection restored Separase protein expression in SiLAT3 treated cells (Figure S8D). These results suggested that LAT3 contributes to the cell cycle of PC through Separase.

LAT3 and Separase expression in prostatectomy specimens and correlation with clinical parameters

To characterize the clinical significance of LAT3, we investigated LAT3 and Separase protein expression in prostatectomy specimens by IHC. The characteristics of all patients and the Kaplan-Meier curve for RFS are summarized in Table 2 and Figure S10, respectively. Both LAT3 and Separase tended to stain weakly in the cancerous areas with Gleason pattern 3 (Fig. 5A to C and D to F), and strongly in the areas with Gleason pattern 4 (Fig. 5G to I and J to L). LAT3 staining was observed at the cell membrane and cytoplasm (Fig. 5C and I) while Separase staining was observed at the nucleus and cytoplasm (Fig. 5F and L). Patients were divided into two groups based on the LAT3 and Separase IHC scores; the median intensity scores were 131 and 171.25, respectively, and 30 (31.91%) patients had high LAT3 and Separase expression while 29 (30.85%) patients had low LAT3 and Separase expression (Fig. 5M). We then designed immunostaining for key genes in the mTOR pathway. Based on previous report[29], we performed immunostaining for p-4EBP1 in prostatectomy specimens and investigated its association with LAT3 expression. As shown in Supplementary figure 11, comparing the LAT3 Low and High groups, the expression of p-4EBP1 was significantly higher

in the High group (P = 0.0228; Fig. S11M).

Next, we investigated the impact of LAT3 and Separase expression on postoperative recurrence. The high LAT3 expression group showed a significantly shorter RFS than the low LAT3 expression group (P = 0.0041; Fig. 5N). Similarly, the Separase high expression group showed a shorter RFS, but the difference was not significant (P = 0.0668; Fig. 5O). Combined analysis of LAT3 and Separase expression demonstrated that the group with high LAT3 and Separase expression had a shorter PFS than the group with low LAT3 and Separase expression (P = 0.0018; Fig. 5P). Similarly, we also performed immunostaining for LAT1 to investigate its association with LAT3 expression and RFS. 19 (20.21%) patients had high LAT3 and LAT1 expression while 19 (20.21%) patients had low LAT3 and LAT1 expression (Fig. S12A). The correlation between LAT3 and LAT1 expression was lower than that between LAT3 and Separase. We also examined the association between LAT1 expression and postoperative recurrence but found no association (P = 0.8472; Fig. S12B).

Next, we investigated the clinical and pathological factors, including the LAT3 and Separase IHC scores, affecting the RFS after prostatectomy. In the univariate Cox proportional hazard model analysis, a high pT stage (hazard ratio (HR): 7.04, P < 0.0001), high LAT3 score (HR: 3.24, P = 0.0018), positive resection margin (HR: 4.44, P < 0.0001), vascular invasion (HR: 6.46, P = 0.0159), and perineural invasion (HR: 2.93, P = 0.0093) were significantly associated with a shorter RFS. In the multivariate analysis, a high pT stage (HR: 4.10, P = 0.0011) and high LAT3 score (HR: 2.46, P = 0.0234) were independent predictive factors for a poor RFS (Table 1).

Finally, we examined the association between LAT3/Separase expression and clinical and pathological factors. High LAT3 expression was significantly associated with a high pT stage (P = 0.0190) and a high International Society of Urological Pathology (ISUP) grade (P =

0.0053; Table S2). High Separase expression was associated with a high ISUP grade ($P < 0.0001$; Table S3).

Discussion

Our study had two major findings. Firstly, we analysed the function of LAT3 in PC. We showed that the expression of LAT3 was regulated by AR, and knockdown of LAT3 suppressed cell proliferation, migration, and invasion *in vitro*. Moreover, high LAT3 expression was correlated with a short RFS after prostatectomy. Secondly, we identified Separase, a protein involved in the cell cycle, as a downstream target of LAT3. High expression of both LAT3 and Separase was correlated with a worse RFS after prostatectomy.

The association between AR, the mTOR pathway and LAT3 has been reported previously by Wang et al[18]. They showed that treatment with BCH (2-aminobicyclo-(2,2,1)-heptane-2-carboxylic acid), a non-specific inhibitor of the LAT family, caused cell cycle arrest in LNCaP cells, and suppressed the phosphorylation of p70S6K, a member of the mTOR pathway. In our study, similar findings were obtained by the knockdown of LAT3 in LNCaP cells. Taken together, these results suggest that LAT3 may play an important role in AR-dependent PC. In addition, LAT3 has also been reported to be associated with epidermal growth factor[30] and oncogenic MYC[31], and further studies are needed.

Recently, another amino acid transporter, LAT1, has been reported to be associated with a variety of cancers[32]. Similar to the present report, the correlation between LAT1 expression and prognosis has been investigated in PC[14], pancreatic cancer[33] and lung cancer[34].

Several groups, including ours, have reported that JPH203, a selective inhibitor of LAT1, interrupts the growth of cancer cells by blocking leucine uptake in various cancer types[19, 20, 35, 36]. The first JPH203 Phase I clinical trial in solid cancer patients was recently conducted [37]. The trial demonstrated modest side effects with long-term disease control in one bile ductal cancer patien[37]. We are currently planning a Phase IIa clinical trial of JPH203 in CRPC patients in whom standard therapy failed. The relationship between cancer and amino acid transporters is expected to be increasingly studied in the future.

Separase is a protease that breaks down chromosomal cohesion during mitosis and plays an essential role in cell cycle progression [38]. Separase has been reported to be overexpressed in human bone, breast, and PC [26]. IHC of patient tissues showed that the expression of Separase was correlated to the prognosis in patients with breast cancer [39] and glioblastoma[27]. In addition, Sepin-1, an inhibitor of Separase, suppressed the cell proliferation, migration, and wound healing of breast cancer cells *in vitro*[40]. In this report, we identified Separase as a downstream target of LAT3; however, the mechanism by which LAT3 knockdown regulates Separase is unknown. Separase may represent a new biomarker or therapeutic target in PC as well as in other cancers.

The results of this study should be considered in light of several limitations. Firstly, no *in vivo* experiments were performed. We do not have the facilities to conduct *in vivo* experiments and are considering collaborating with other institutions. Instead, to obtain supportive evidence, we thoroughly studied the clinical significance of LAT3 in PC patients. Secondly, the study cohort used to investigate the LAT3 expression profile was quite small. We are planning a larger multi-institutional study to assess the prognostic value of LAT3 in PC patients. Thirdly, we analysed the expression of LAT3 only in patients who had received a prostatectomy. We are currently planning a prospective clinical trial that includes patients with

CRPC and neuroendocrine PC.

In summary, LAT3 expression was regulated by AR in PC cells, and high LAT3 expression correlated with a poor prognosis after prostatectomy. Knockdown of LAT3 suppressed the proliferative activities of PC cells and arrested the cell cycle. We identified Separase, which is involved in the cell cycle, as a downstream target of LAT3. LAT3 and Separase may serve as prognostic markers and therapeutic targets in hormone-sensitive PC.

Acknowledgements

The authors thank Dr. Osamu Ohara (Kazusa DNA Research Institute, Kisarazu, Japan) for the RNA-seq analysis. The authors also thank Hisayo Karahi, Miyuki Yamaguchi, and Natsuko Kusama (Experimental Assistants, Chiba University) for their support of this study. The present work was supported by a Grant-in-Aid for Scientific Research (B) (grant #20H03813) to TI, and a Grant-in-Aid for Scientific Research (C) (grant #20K09555) to SS.

Disclosure statement

The authors declare no conflicts of interest.

References

1 Barsouk A, Padala SA, Vakiti A, et al. Epidemiology, Staging and Management of Prostate Cancer. *Medical sciences (Basel, Switzerland)*. 2020; 8.

2 Shore ND, Morgans AK, Ryan CJ. Resetting the Bar of Castration Resistance - Understanding Androgen Dynamics in Therapy Resistance and Treatment Choice in Prostate Cancer. *Clinical*

genitourinary cancer. 2020.

3 Feldman BJ, Feldman D. The development of androgen-independent prostate cancer. *Nature reviews Cancer*. 2001; 1: 34-45.

4 Yamada Y, Sakamoto S, Rii J, et al. How many bone metastases may be defined as high-volume metastatic prostate cancer in Asians: A retrospective multicenter cohort study. *Prostate*. 2020; 80: 432-440.

5 Yamada Y, Sakamoto S, Rii J, et al. Prognostic value of an inflammatory index for patients with metastatic castration-resistant prostate cancer. *Prostate*. 2020; 80: 559-569.

6 Ando K, Sakamoto S, Takeshita N, et al. Higher serum testosterone levels predict poor prognosis in castration-resistant prostate cancer patients treated with docetaxel. *Prostate*. 2020; 80: 247-255.

7 Rii J, Sakamoto S, Yamada Y, et al. Prognostic factors influencing overall survival in de novo oligometastatic prostate cancer patients. *Prostate*. 2020; 80: 850-858.

8 Sakamoto S, Maimaiti M, Xu M, et al. Higher Serum Testosterone Levels Associated with Favorable Prognosis in Enzalutamide- and Abiraterone-Treated Castration-Resistant Prostate Cancer. *Journal of clinical medicine*. 2019; 8.

9 Obinata D, Lawrence MG, Takayama K, et al. Recent Discoveries in the Androgen Receptor Pathway in Castration-Resistant Prostate Cancer. *Frontiers in oncology*. 2020; 10: 581515.

10 Sugiura M, Sato H, Okabe A, et al. Identification of AR-V7 downstream genes commonly targeted by AR/AR-V7 and specifically targeted by AR-V7 in castration resistant prostate cancer. *Translational oncology*. 2020; 14: 100915.

11 Sugiura M, Sato H, Kanesaka M, et al. Epigenetic modifications in prostate cancer. *Int J Urol*. 2020.

12 Sakamoto S. Current status of circulating tumor cell androgen receptor splice variant-7 in metastatic castration-resistant prostate cancer. *Annals of translational medicine*. 2019; 7: S375.

13 Bröer S. Amino Acid Transporters as Targets for Cancer Therapy: Why, Where, When, and How. *International journal of molecular sciences*. 2020; 21.

14 Xu M, Sakamoto S, Matsushima J, et al. Up-Regulation of LAT1 during Antiandrogen Therapy Contributes to Progression in Prostate Cancer

Cells. *The Journal of urology*. 2016; 195: 1588-1597.

15 Wang Q, Holst J. L-type amino acid transport and cancer: targeting the mTORC1 pathway to inhibit neoplasia. *American journal of cancer research*. 2015; 5: 1281-1294.

16 Cole KA, Chuaqui RF, Katz K, et al. cDNA sequencing and analysis of POV1 (PB39): a novel gene up-regulated in prostate cancer. *Genomics*. 1998; 51: 282-287.

17 Babu E, Kanai Y, Chairoungdua A, et al. Identification of a novel system L amino acid transporter structurally distinct from heterodimeric amino acid transporters. *J Biol Chem*. 2003; 278: 43838-43845.

18 Wang Q, Bailey CG, Ng C, et al. Androgen receptor and nutrient signaling pathways coordinate the demand for increased amino acid transport during prostate cancer progression. *Cancer Res*. 2011; 71: 7525-7536.

19 Maimaiti M, Sakamoto S, Yamada Y, et al. Expression of L-type amino acid transporter 1 as a molecular target for prognostic and therapeutic indicators in bladder carcinoma. *Scientific reports*. 2020; 10: 1292.

20 Higuchi K, Sakamoto S, Ando K, et al. Characterization of the expression of LAT1 as a prognostic indicator and a therapeutic target in renal cell carcinoma. *Scientific reports*. 2019; 9: 16776.

21 Goto Y, Kojima S, Kurozumi A, et al. Regulation of E3 ubiquitin ligase-1 (WWP1) by microRNA-452 inhibits cancer cell migration and invasion in prostate cancer. *British journal of cancer*. 2016; 114: 1135-1144.

22 Zhou Y, Zhou B, Pache L, et al. Metascape provides a biologist-oriented resource for the analysis of systems-level datasets. *Nature communications*. 2019; 10: 1523.

23 Grasso CS, Wu YM, Robinson DR, et al. The mutational landscape of lethal castration-resistant prostate cancer. *Nature*. 2012; 487: 239-243.

24 Luo JH, Yu YP, Cieply K, et al. Gene expression analysis of prostate cancers. *Molecular carcinogenesis*. 2002; 33: 25-35.

25 Imamura Y, Sakamoto S, Endo T, et al. FOXA1 promotes tumor progression in prostate cancer via the insulin-like growth factor binding protein 3 pathway. *PloS one*. 2012; 7: e42456.

26 Meyer R, Fofanov V, Panigrahi A, Merchant F, Zhang N, Pati D.

Overexpression and mislocalization of the chromosomal segregation protein separase in multiple human cancers. *Clinical cancer research : an official journal of the American Association for Cancer Research*. 2009; 15: 2703-2710.

27 Mukherjee M, Byrd T, Brawley VS, et al. Overexpression and constitutive nuclear localization of cohesin protease Separase protein correlates with high incidence of relapse and reduced overall survival in glioblastoma multiforme. *Journal of neuro-oncology*. 2014; 119: 27-35.

28 Zhang N, Scorsone K, Ge G, et al. Identification and Characterization of Separase Inhibitors (Sepins) for Cancer Therapy. *Journal of biomolecular screening*. 2014; 19: 878-889.

29 Chen X, Xiong X, Cui D, et al. DEPTOR is an in vivo tumor suppressor that inhibits prostate tumorigenesis via the inactivation of mTORC1/2 signals. *Oncogene*. 2020; 39: 1557-1571.

30 Zhang BK, Moran AM, Bailey CG, Rasko JEJ, Holst J, Wang Q. EGF-activated PI3K/Akt signalling coordinates leucine uptake by regulating LAT3 expression in prostate cancer. *Cell Commun Signal*. 2019; 17: 83.

31 Yue M, Jiang J, Gao P, Liu H, Qing G. Oncogenic MYC Activates a Feedforward Regulatory Loop Promoting Essential Amino Acid Metabolism and Tumorigenesis. *Cell Rep*. 2017; 21: 3819-3832.

32 Puris E, Gynther M, Auriola S, Huttunen KM. L-Type amino acid transporter 1 as a target for drug delivery. *Pharmaceutical research*. 2020; 37: 88.

33 Kaira K, Arakawa K, Shimizu K, et al. Relationship between CD147 and expression of amino acid transporters (LAT1 and ASCT2) in patients with pancreatic cancer. *American journal of translational research*. 2015; 7: 356-363.

34 Kaira K, Kawashima O, Endoh H, et al. Expression of amino acid transporter (LAT1 and 4F2hc) in pulmonary pleomorphic carcinoma. *Human pathology*. 2019; 84: 142-149.

35 Yun DW, Lee SA, Park MG, et al. JPH203, an L-type amino acid transporter 1-selective compound, induces apoptosis of YD-38 human oral cancer cells. *Journal of pharmacological sciences*. 2014; 124: 208-217.

36 Cormerais Y, Giuliano S, LeFloch R, et al. Genetic Disruption of the

Multifunctional CD98/LAT1 Complex Demonstrates the Key Role of Essential Amino Acid Transport in the Control of mTORC1 and Tumor Growth. *Cancer Res*. 2016; 76: 4481-4492.

37 Okano N, Naruge D, Kawai K, et al. First-in-human phase I study of JPH203, an L-type amino acid transporter 1 inhibitor, in patients with advanced solid tumors. *Investigational new drugs*. 2020; 38: 1495-1506.

38 Zhang N, Pati D. Biology and insights into the role of cohesin protease separase in human malignancies. *Biological reviews of the Cambridge Philosophical Society*. 2017; 92: 2070-2083.

39 Gurvits N, Löyttyniemi E, Nykänen M, Kuopio T, Kronqvist P, Talvinen K. Separase is a marker for prognosis and mitotic activity in breast cancer. *British journal of cancer*. 2017; 117: 1383-1391.

40 Zhang N, Pati D. Separase Inhibitor Sepin-1 Inhibits Foxm1 Expression and Breast Cancer Cell Growth. *Journal of cancer science & therapy*. 2018; 10.

Figure legends

Figure 1. Quantification of LAT3 expression and regulation by AR. (A) *LAT3* mRNA levels of human PC cells in FBS or CSS were analysed by RT-PCR. (B) LAT3 protein levels were analysed by western blotting. GAPDH was used as a loading control. (C and D) Effect of DHT and bicalutamide on LAT3 expression in LNCaP (C) and C4-2 (D) cells. (E and F) Comparison of the LAT3 and AR protein expression levels in LNCaP (E) and C4-2 (F) cells treated with DHT and/or bicalutamide (Bic). Each bar represents the mean with the standard error of the mean (S.E.M.). *P < 0.05, **P < 0.01, N.S.: not significant (unpaired Student's t-test).

Figure 2. Inhibition of LAT3 expression and the mTOR pathway by AR and LAT3 knockdown, and the chromatin immunoprecipitation sequencing assay of AR. (A and C) Changes in *LAT3* and *AR* mRNA expression due to SiAR in LNCaP (A) and C4-2 (C) cells. (B and D) Decreases in the LAT3 and AR protein expression due to SiAR in LNCaP (B) and C4-2 (D) cells. (E) Changes in

LAT3 and AR expression over time with CSS administration. (F) Epigenetic status around the *LAT3* locus in the genome browser view. AR binding to LAT3 (SLC43A1) in DHT-stimulated LNCaP cells. (G and H) Confirmation of the LAT3-knockdown effect of SiLAT3 in LNCaP (G) and C4-2 (H) cells. (I) Effect of SiLAT3 on the phosphorylation status of the mTOR signalling pathway in LNCaP and C4-2 cells. GAPDH was used as a loading control. Each bar represents the mean with the S.E.M. Sinega: siRNA negative control, *P < 0.05, **P < 0.01, N.S.: not significant (unpaired Student's t-test).

Figure 3. Effects of SiLAT3 on the cell viability, migration, and invasion of PC cells. (A, D, G) SiLAT3 significantly reduced the cell proliferation in LNCaP cells (A) and C4-2 cells in FBS (G), but not C4-2 cells in CSS (D). (B, E, H) Transwell chamber migration assays were used to evaluate the migratory changes in LNCaP cells (B), C4-2 cells in CSS (E), and C4-2 cells in FBS (H). (C, F, I) Matrigel invasion assays were used to evaluate the invasion activities of LNCaP cells (C), C4-2 cells in CSS (F), and C4-2 cells in FBS (I). Representative images of three independent experiments are shown. Each bar represents the mean with the S.E.M. Sinega: siRNA negative control, **P < 0.01, N.S.: not significant (unpaired Student's t-test).

Figure 4. Identification of Separase (*ESPL1*) as a downstream target of LAT3. (A) The genes downregulated by SiLAT3 were significantly associated with gene ontology (GO) terms such as "cell cycle", "DNA replication", and "cell division". (B) The top 10 genes that were downregulated by SiLAT3 are listed. (C) The mRNA expression level of downregulated genes was evaluated by RT-PCR. (D) Western blotting results showing that the Separase protein expression level was decreased by SiLAT3. (E) Cell cycle analysis. A remarkable decrease in the number of cells in the S phase and G2/M phase, and an increase of cells in the G0/G1 phase are

seen. (F) LNCaP cells were treated with various concentrations of Sepin-1, a selective Separase inhibitor, for 72 hr. Viability curves are shown as a percentage of the control values, which were acquired from cells treated with dimethyl sulfoxide (0.5%). (G) The relationship between the Separase inhibitor dose and LNCaP cell viability. (H) Validation of the additive effects of Separase inhibitors and AR inhibitors on LNCaP cell proliferation. The data represent the results from three independent experiments. *P < 0.05, **P < 0.01 (unpaired Student's t-test).

Figure 5. Immunostaining for LAT3 and Separase in prostatectomy specimens, and their relation to clinicopathological factors. (A-L) Representative images of LAT3 immunostaining in areas with Gleason pattern 3 (A to C) and pattern 4 (G to I), and of Separase immunostaining in areas with Gleason pattern 3 (D to F) and pattern 4 (J to L). (M) Venn diagram of the distribution of the number of patients with high and/or low LAT3 and Separase scores. (N) Kaplan-Meier analysis of RFS according to high or low LAT3 scores. (O) Kaplan-Meier analysis of RFS according to high or low Separase scores. (P) Kaplan-Meier analysis of RFS according to high LAT3 and high Separase scores, low LAT3 and low Separase scores, or others. The P value was calculated by the log-rank test.

Supporting information

Figure S1. Original full images of the western blots used in Figure 1. (A) Western blot image of LAT3 and GAPDH in various PC cells. (B) Western blot image of LAT3 and GAPDH in LNCaP and C4-2 cells. (C) Western blot image of LAT3, AR, and GAPDH in LNCaP cells treated with various serum conditions. (D) Western blot image of LAT3, AR, and GAPDH in C4-2 cells treated with various serum conditions.

Figure S2. Original full western blot images used in Figure 2. (A) Western blot image of LAT3, AR, and GAPDH in LNCaP and C4-2 cells treated with SiAR. (B) Western blot image of LAT3, AR, and GAPDH in LNCaP cells treated with CSS. (C) Western blot image of LAT3, AR, and GAPDH in LNCaP and C4-2 cells treated with SiLAT3.

Figure S3. Original full western blot images used in Figure 3. (A) Western blot image of LAT3, mTOR pathway proteins, and GAPDH in LNCaP cells treated with SiLAT3. (B) Western blot image of Separase in LNCaP cells treated with SiLAT3.

Figure S4. LAT3 expression in clinical datasets. (A) LAT3 expression levels in normal prostate tissue and PC (Luo dataset). (B) LAT3 expression levels in normal prostate tissue, localized PC, and CRPC (Grasso dataset). (C) LAT3 expression levels in PC with or without AR amplification (Grasso dataset). **P < 0.01, N.S.: not significant (unpaired Student's t-test).

Figure S5. Epigenetic status around the *LAT3* locus in the genome browser view. AR-halfsite motif is shown.

Figure S6. Effect of SiAR on the phosphorylation status of the mTOR signalling pathway in LNCaP and C4-2 cells. GAPDH was used as a loading control.

Figure S7. Effects of SiLAT3 on the wound healing and the expression of EMT-related proteins in PC cells. (A to C) SiLAT3 significantly reduced the wound healing in LNCaP cells (A) and C4-2 cells in FBS (C), but not C4-2 cells in CSS (B). (D) Effect of SiLAT3 on the expression of EMT-related proteins in LNCaP and C4-2 cells. GAPDH was used as a loading control.

Figure S8. Knock down and rescue effect of LAT3 or Separase on cell proliferation. (A) Knock down and rescue effect o LAT3 vector on cell proliferation. (B) Effect of MDV3100 and LAT3 vector on the expression of LAT3 in LNCaP cells. GAPDH was used as a loading control. (C) Knock down and rescue effect o Separase vector on cell proliferation. (D) Effect of SiLAT3 and Separase vector on the expression of LAT3 in LNCaP cells. GAPDH was used as a loading control. Sinega: siRNA negative control, *P < 0.05, **P < 0.01.

Figure S9. Validation of the additive effect of Separase inhibitor and AR inhibitor on LNCaP cell proliferation. (A) Additive effect of Sepin-1 on apautamide. (B) Additive effect of Sepin-1 on CSS medium. *P < 0.05, **P < 0.01 (unpaired Student's t-test).

Figure S10. Kaplan-Meier analysis of RFS in all patients.

Figure S11. Immunostaining for LAT3 and p-4EBP1 in prostatectomy specimens, and their relationship. (A-L) Representative images of LAT3 immunostaining of patient in LAT3 Low group (A to C) and High group (D to F), and of p-4EBP1 immunostaining of patient in LAT3 Low group (G to I) and High group (J to L). (M) Comparison of p-4EBP1 IHC score of LAT3 Low and High group.

Figure S12. Relationship of IHC score between LAT3 and LAT1. (A) Venn diagram of the distribution of the number of patients with high and/or low LAT3 and LAT1 scores. (B) Kaplan-Meier analysis of RFS according to high or low LAT3 scores. The P value was calculated by the log-rank test.

Table S1. Primer sequences for RT-PCR.

Table S2. Characteristics of low and high LAT3 groups.

Table S3. Characteristics of low and high Separase groups.

Figure 1

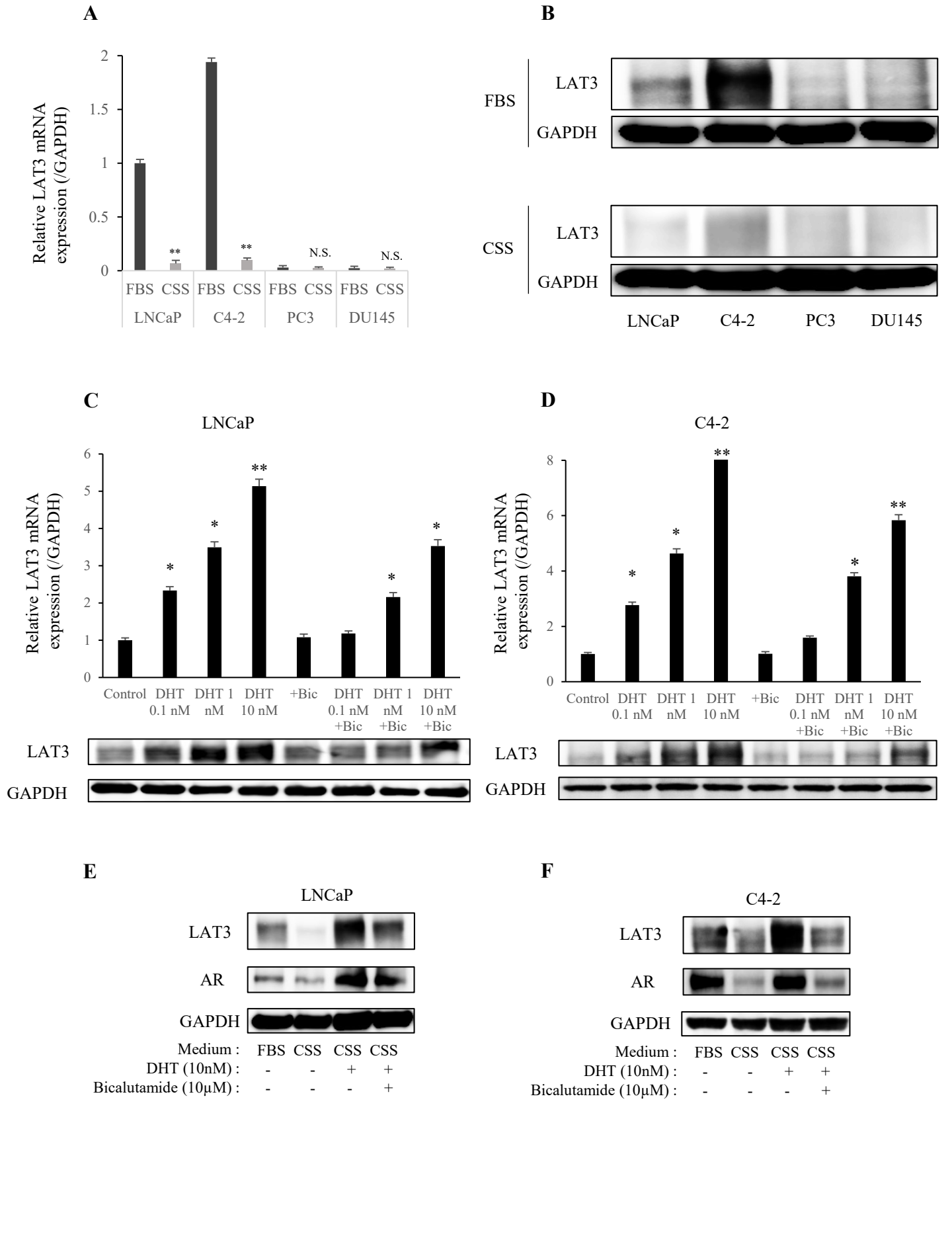
A
Relative LAT3 mRNA expression (/GAPDH)
2
1.5
1
0.5
0
**
**
N.S.
N.S.
FBS CSS FBS CSS FBS CSS FBS CSS
LNCaP C4-2 PC3 DU145
B
FBS
LAT3
GAPDH
CSS
LAT3
GAPDH
LNCaP C4-2 PC3 DU145
C
LNCaP
Relative LAT3 mRNA expression (/GAPDH)
Control DHT 0.1 nM DHT 1 nM DHT 10 nM +Bic DHT 0.1 nM +Bic DHT 1 nM +Bic DHT 10 nM +Bic
LAT3
GAPDH
D
C4-2
Relative LAT3 mRNA expression (/GAPDH)
Control DHT 0.1 nM DHT 1 nM DHT 10 nM +Bic DHT 0.1 nM +Bic DHT 1 nM +Bic DHT 10 nM +Bic
LAT3
GAPDH
E
LNCaP
LAT3
AR
GAPDH
Medium : FBS CSS CSS CSS
DHT (10nM) : - - + +
Bicalutamide (10μM) : - - - +
F
C4-2
LAT3
AR
GAPDH
Medium : FBS CSS CSS CSS
DHT (10nM) : - - + +
Bicalutamide (10μM) : - - - +

Figure 2

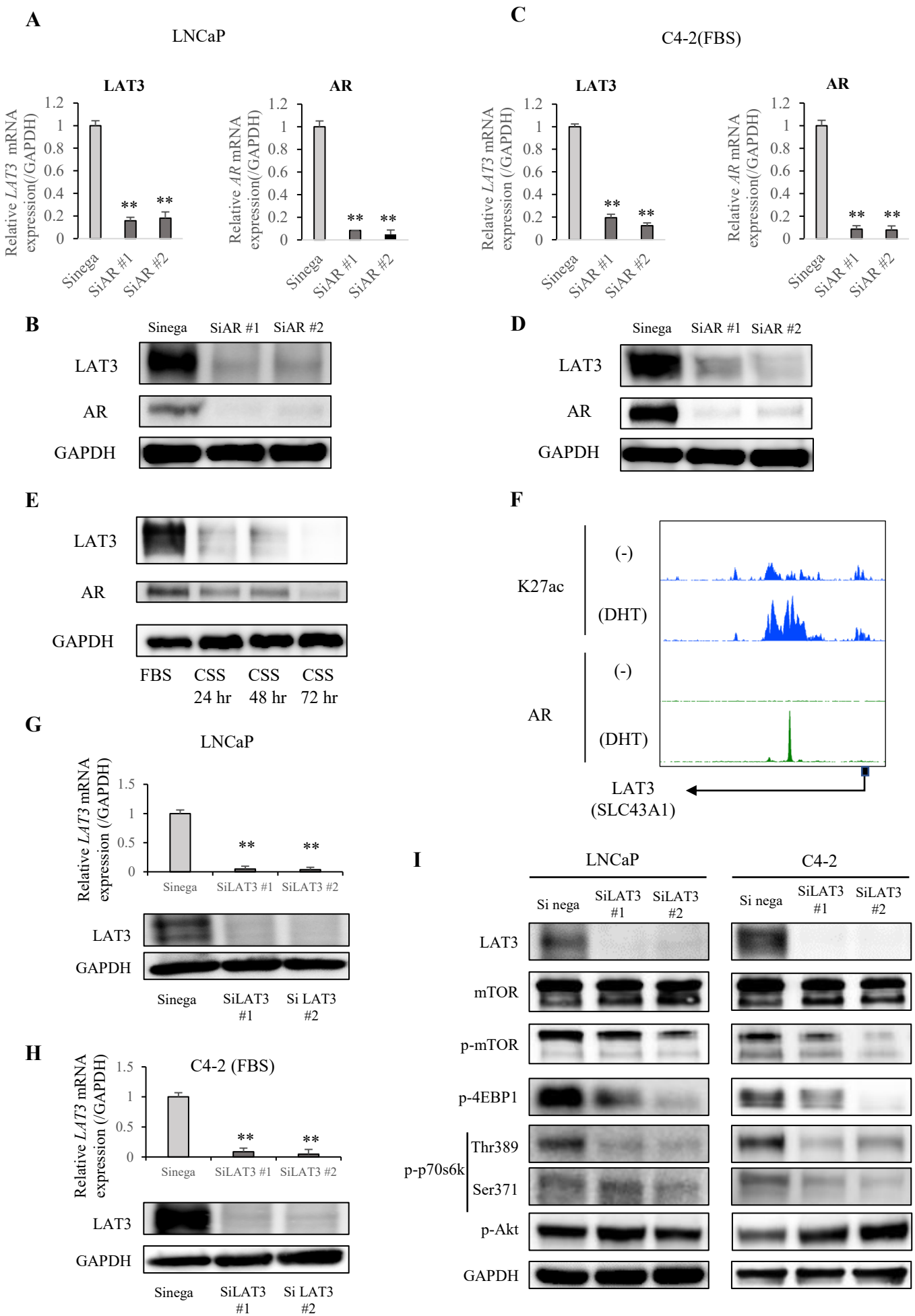
A
LNCaP
LAT3
AR
Relative LAT3 mRNA expression(/GAPDH)
Relative AR mRNA expression(/GAPDH)
Sinega
SiAR #1
SiAR #2
B
Sinega
SiAR #1
SiAR #2
LAT3
AR
GAPDH
C
C4-2(FBS)
D
E
FBS
CSS 24 hr
CSS 48 hr
CSS 72 hr
F
K27ac
AR
(-)
(DHT)
LAT3 (SLC43A1)
G
LNCaP
Relative LAT3 mRNA expression (/GAPDH)
SiLAT3 #1
SiLAT3 #2
Si LAT3 #2
H
C4-2 (FBS)
I
LNCaP
C4-2
Si nega
SiLAT3 #1
SiLAT3 #2
mTOR
p-mTOR
p-4EBP1
p-p70s6k
Thr389
Ser371
p-Akt

Figure 3

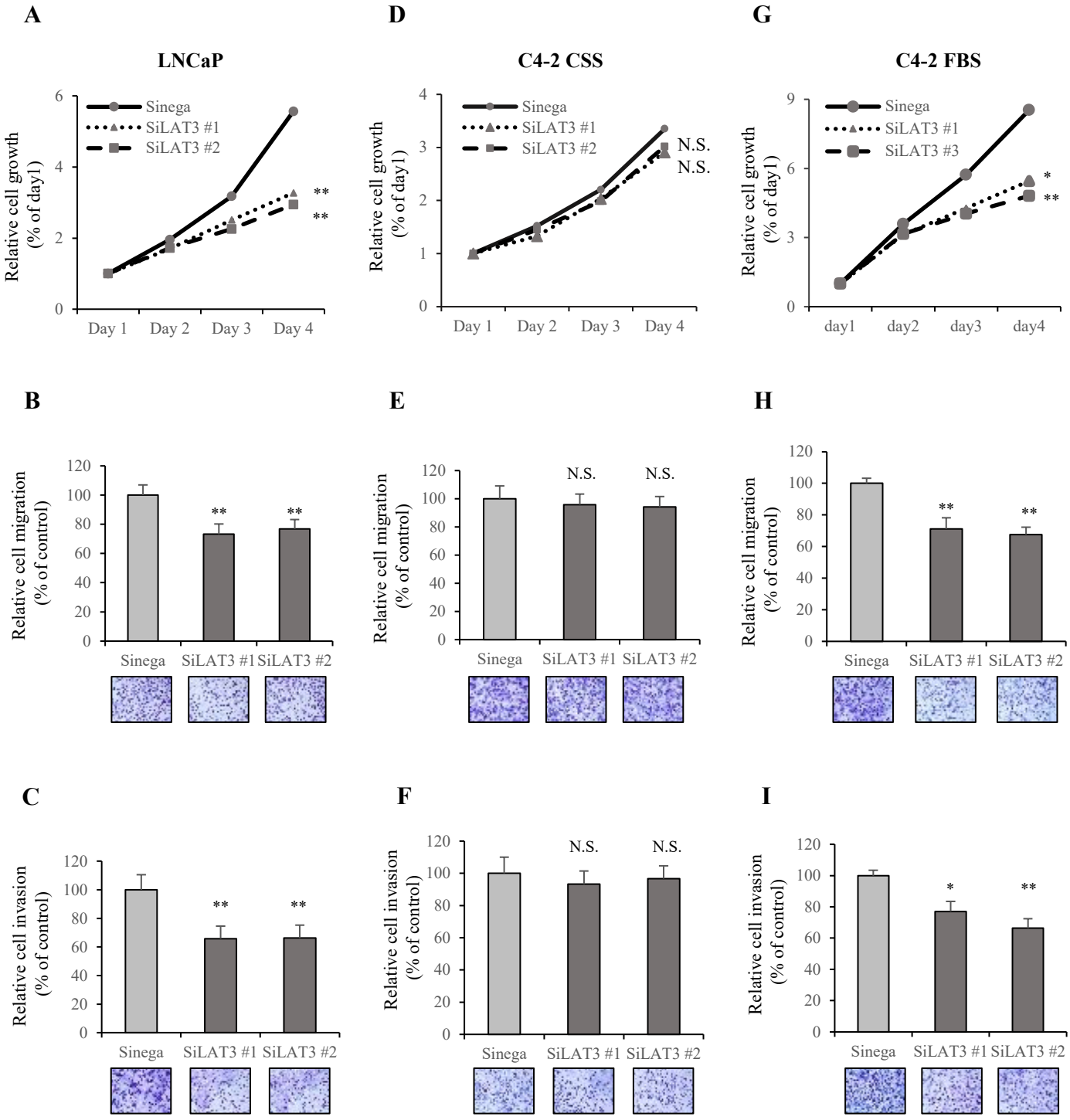
A
LNCaP
Relative cell growth (% of day1)
Sinega
SiLAT3 #1
SiLAT3 #2
Day 1
Day 2
Day 3
Day 4
**
**
D
C4-2 CSS
Relative cell growth (% of day1)
Sinega
SiLAT3 #1
SiLAT3 #2
N.S.
N.S.
Day 1
Day 2
Day 3
Day 4
G
C4-2 FBS
Relative cell growth (% of day1)
Sinega
SiLAT3 #1
SiLAT3 #3
*
**
day1
day2
day3
day4
B
Relative cell migration (% of control)
**
**
Sinega
SiLAT3 #1
SiLAT3 #2
E
Relative cell migration (% of control)
N.S.
N.S.
Sinega
SiLAT3 #1
SiLAT3 #2
H
Relative cell migration (% of control)
**
**
Sinega
SiLAT3 #1
SiLAT3 #2
C
Relative cell invasion (% of control)
**
**
Sinega
SiLAT3 #1
SiLAT3 #2
F
Relative cell invasion (% of control)
N.S.
N.S.
Sinega
SiLAT3 #1
SiLAT3 #2
I
Relative cell invasion (% of control)
*
**
Sinega
SiLAT3 #1
SiLAT3 #2

Figure 4

A

GO analysis in downregulated genes by SiLAT3

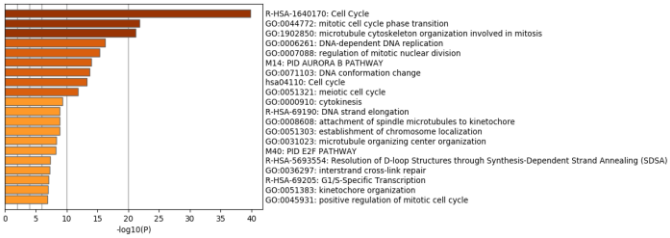

B

Downregulated gene list by SiLAT3

Gene name	Log
PGC	-2.74051
LAT3	**-2.58398**
CLEC7A	-2.4061
ESCO2	-2.35089
LNPEP	-2.31415
Separase	**-2.28594**
LAMA1	-2.20899
NMU	-2.0748
ACBD7	-1.99581
EFCC1	-1.99374

C

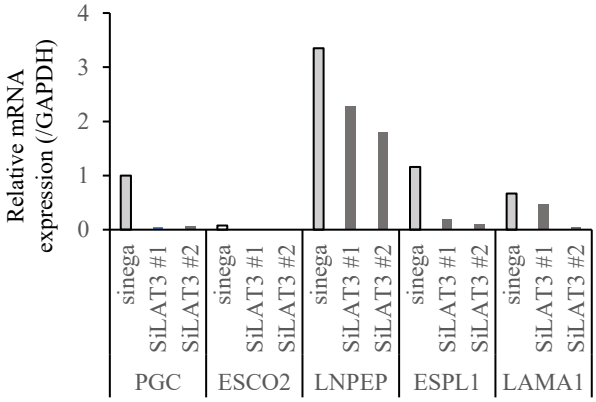

D

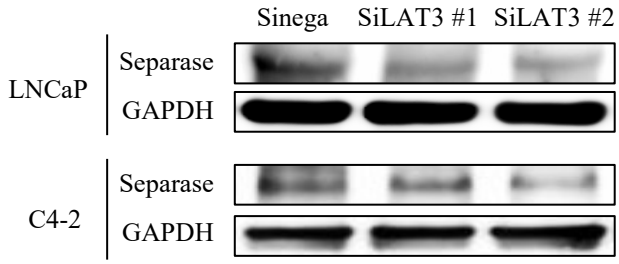

E

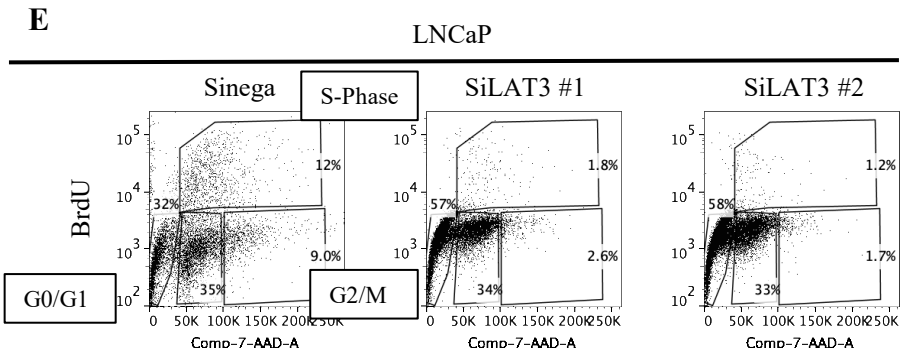

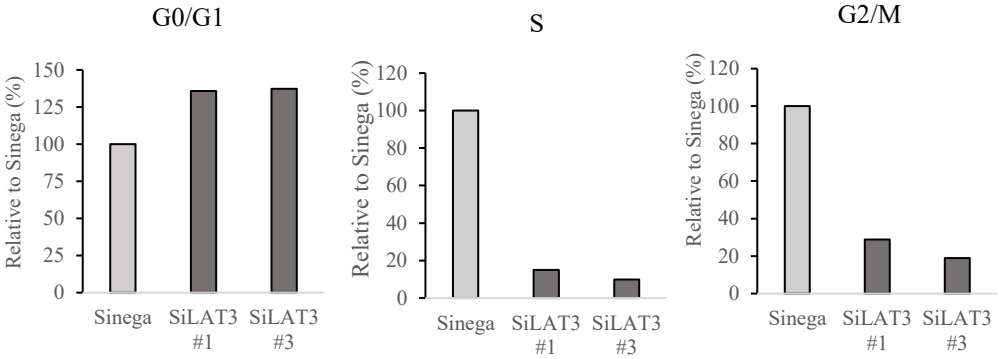

F

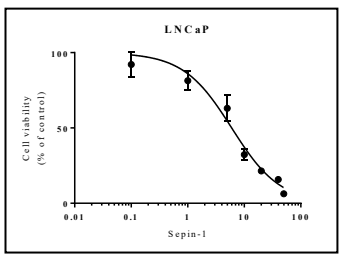

IC50 : 5.99μM ± 1.195 (95% CI)

G

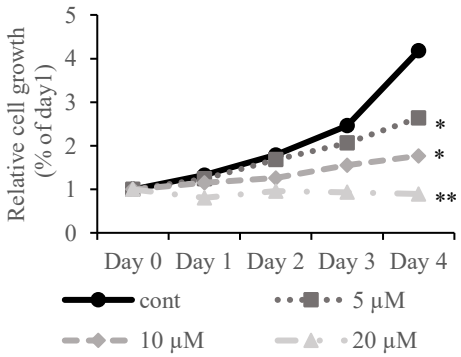

H

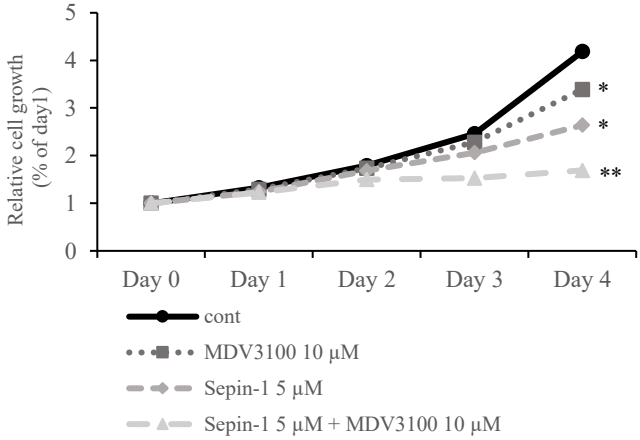

Figure 5

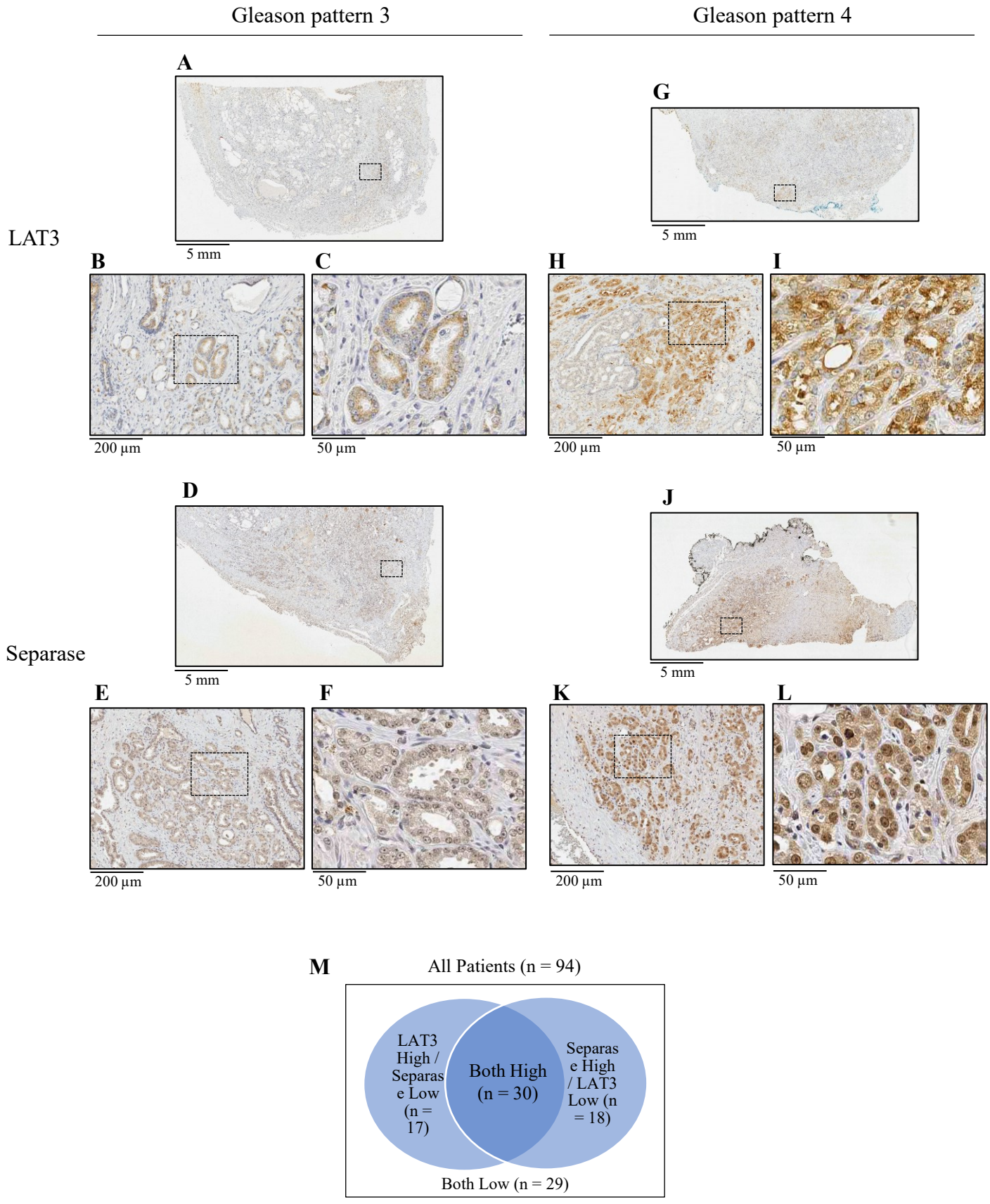
Gleason pattern 3
Gleason pattern 4
LAT3
Separase
A
B
C
D
E
F
G
H
I
J
K
L
5 mm
200 µm
50 µm
M
All Patients (n = 94)
LAT3 High / Separase Low (n = 17)
Both High (n = 30)
Separase High / LAT3 Low (n = 18)
Both Low (n = 29)

N

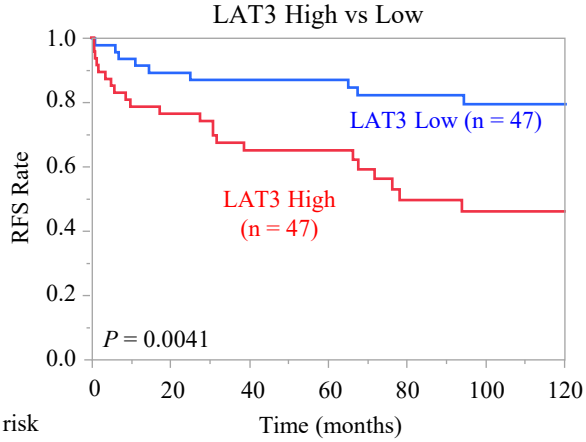

No. at risk						
LAT3 Low	47	42	38	37	34	26
LAT3 High	47	35	28	23	16	13

O

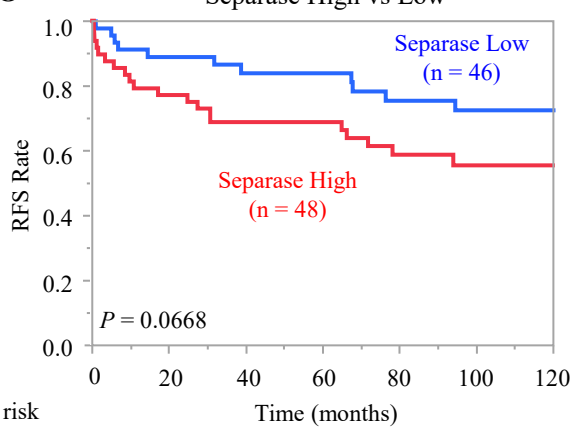

No. at risk						
Separase Low	46	39	32	30	27	25
Separase High	48	38	33	30	23	16

P

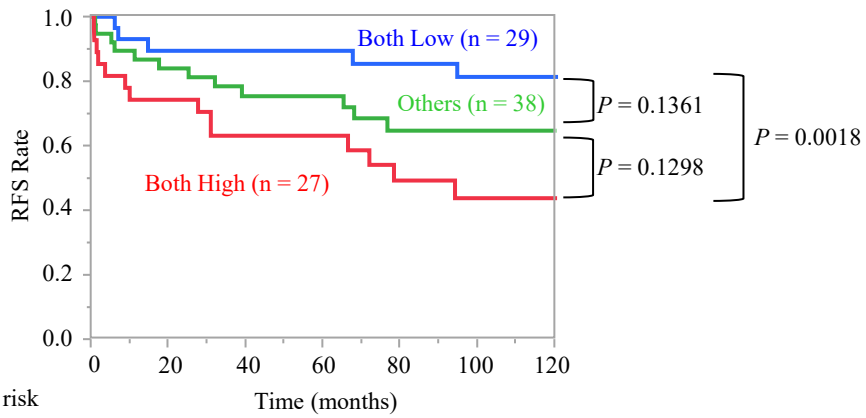

No. at risk						
Both Low	29	25	23	22	21	20
Others	38	31	25	23	18	13
Both High	27	20	17	15	11	9

Figure S1

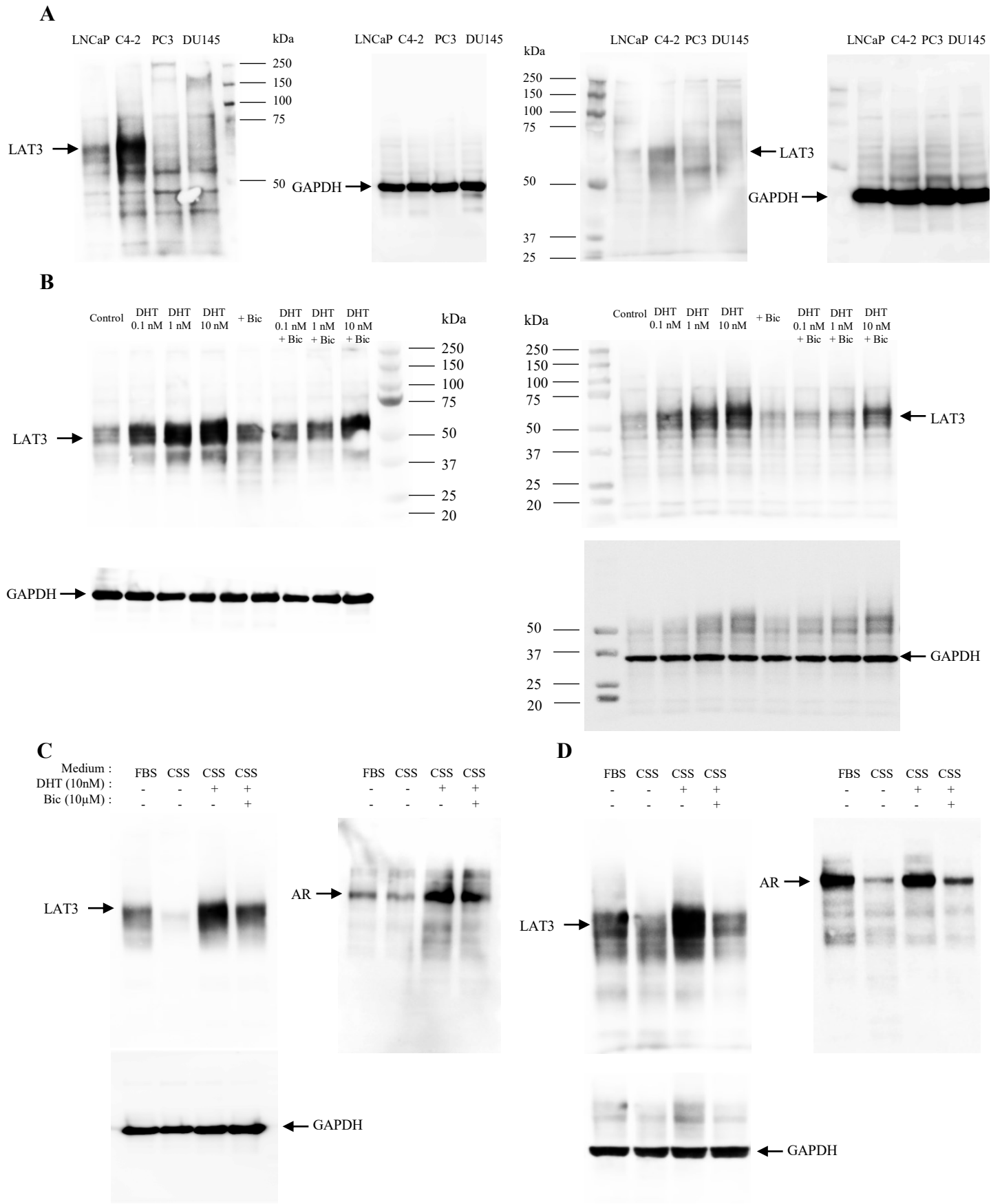

Figure S1. Original full images of the western blots used in Figure 1.
(A) Western blot image of LAT3 and GAPDH in various PC cells. (B) Western blot image of LAT3 and (B) GAPDH in LNCaP and C4-2 cells. (C) Western blot image of LAT3, AR, and GAPDH in LNCaP cells (C) treated with various serum conditions. (D) Western blot image of LAT3, AR, and GAPDH in C4-2 cells (D) treated with various serum conditions.

Figure S2

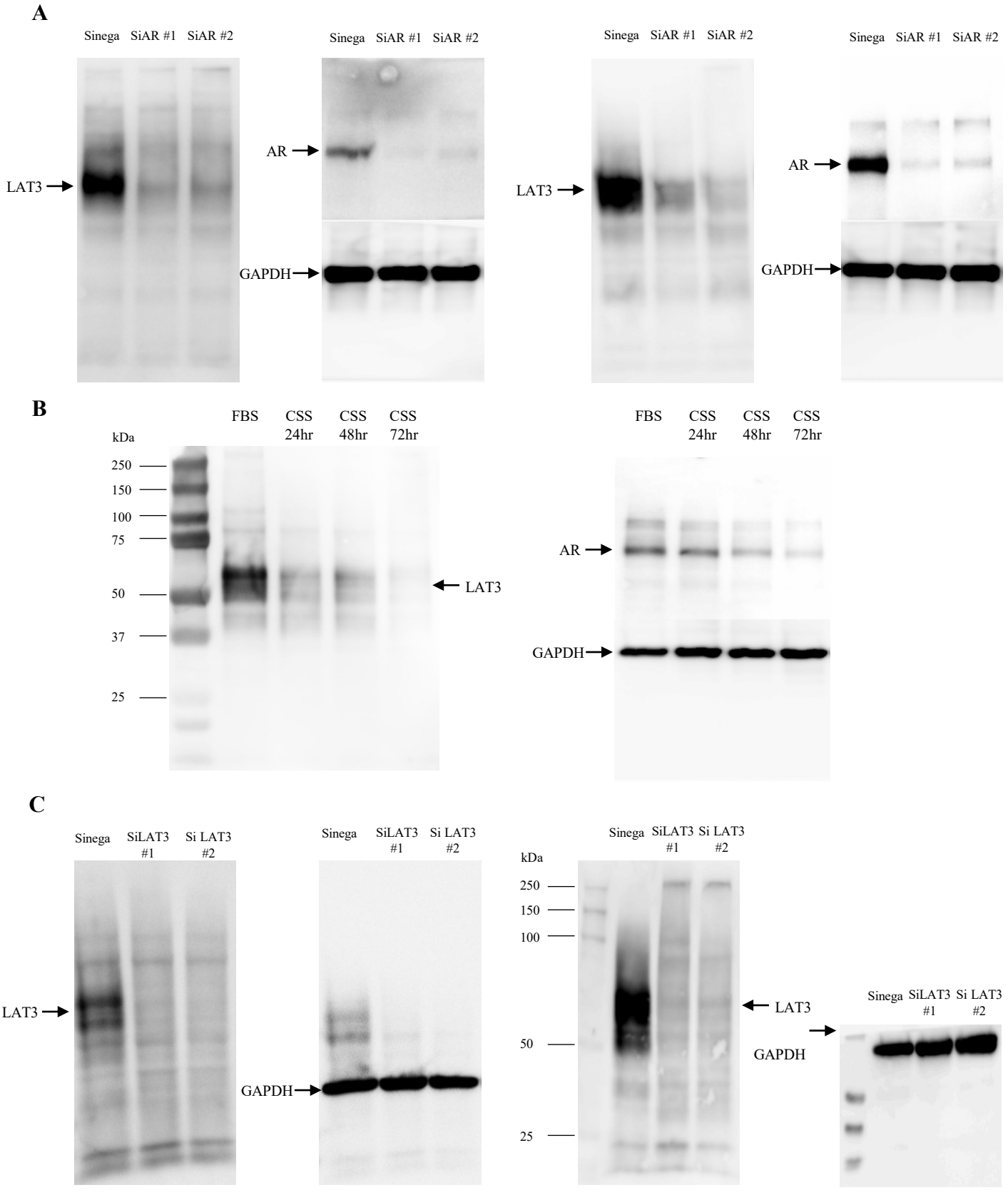

Figure S2. Original full western blot images used in Figure 2.
(A) Western blot image of LAT3, AR, and GAPDH in LNCaP and C4-2 cells treated with SiAR.
(B) Western blot image of LAT3, AR, and GAPDH in LNCaP cells treated with CSS.
(C) Western blot image of LAT3, AR, and GAPDH in LNCaP and C4-2 cells treated with SiLAT3.

Figure S3

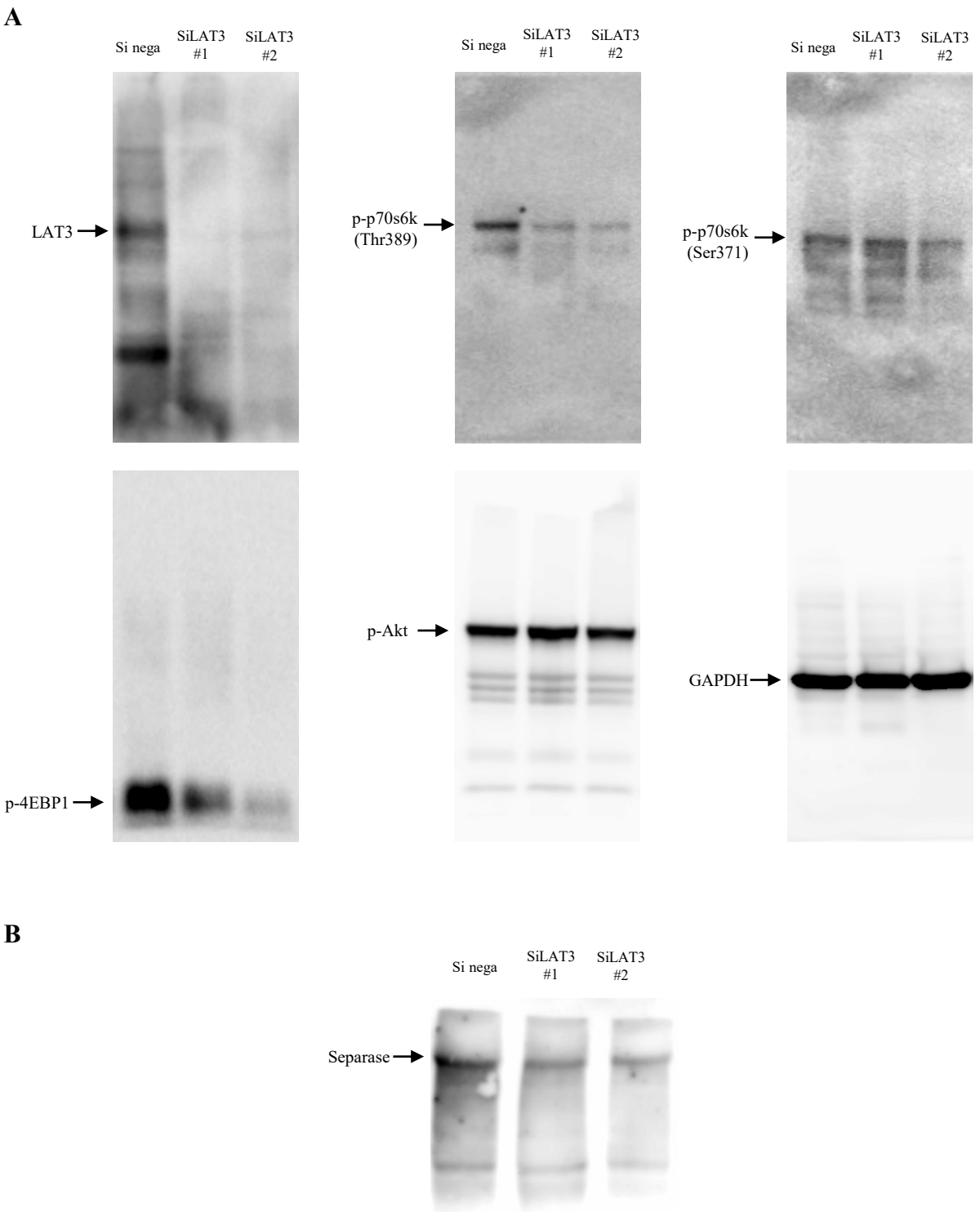

Figure S3. Original full western blot images used in Figure 3.
(A) Western blot image of LAT3, mTOR pathway proteins, and GAPDH in LNCaP cells treated with SiLAT3. (B) Western blot image of Separase in LNCaP cells treated with SiLAT3.

Figure S4

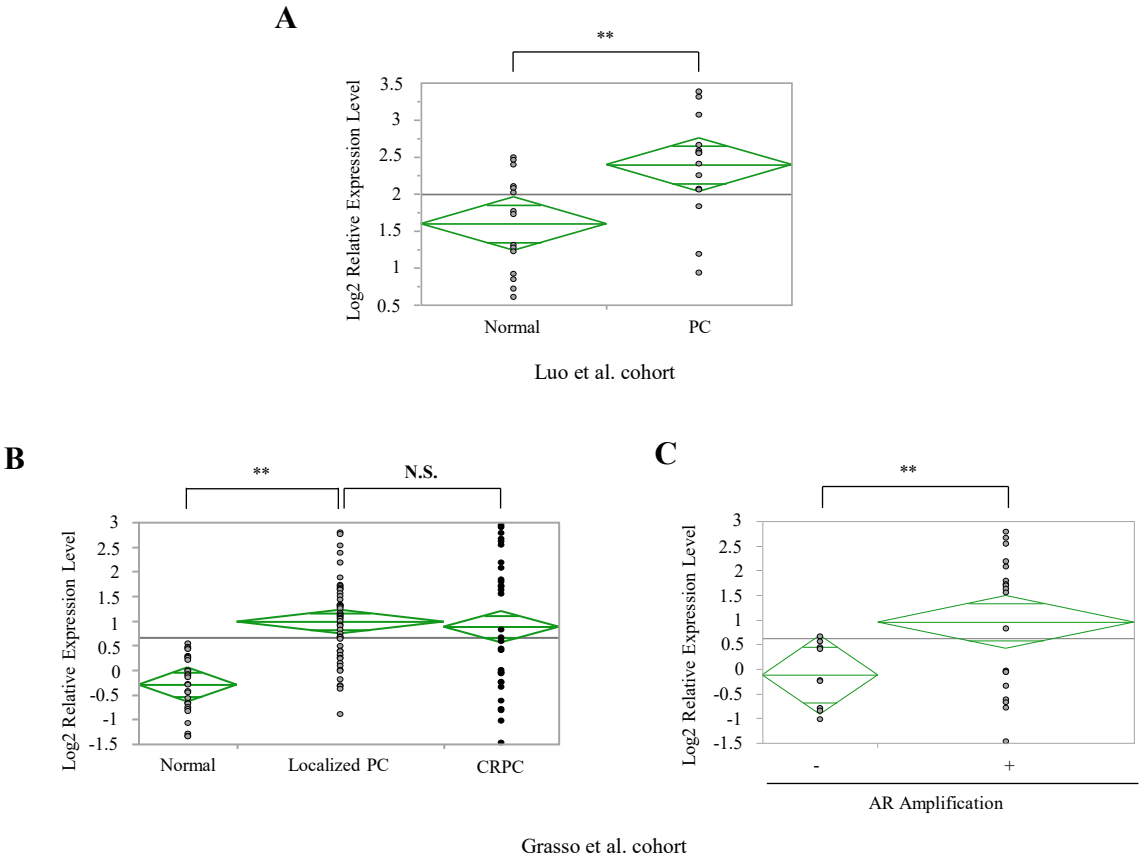

Figure S4. LAT3 expression in clinical datasets.

(A) LAT3 expression levels in normal prostate tissue and PC (Luo dataset). (B) LAT3 expression levels in normal prostate tissue, localized PC, and CRPC (Grasso dataset). (C) LAT3 expression levels in PC with or without AR amplification (Grasso dataset). **P < 0.01, N.S.: not significant (unpaired Student's t-test).

Figure S5

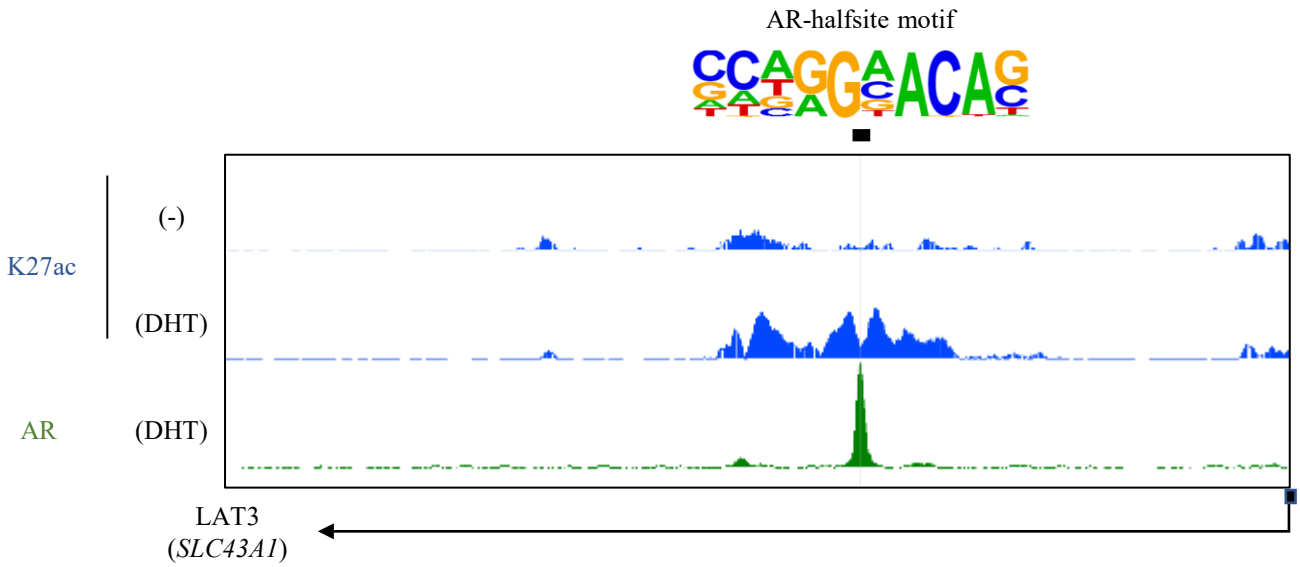

Figure S5. Epigenetic status around the *LAT3* locus in the genome browser view.
AR-halfsite motif is shown.

Figure S6

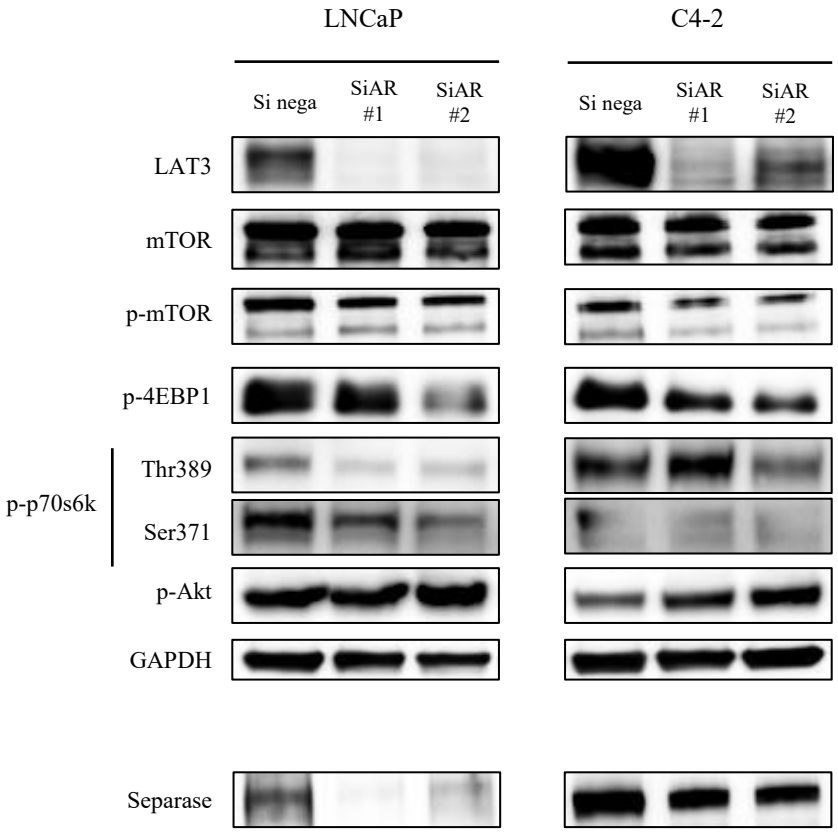

Figure S6. Effect of SiAR on the phosphorylation status of the mTOR signalling pathway in LNCaP and C4-2 cells.
GAPDH was used as a loading control.

Figure S7

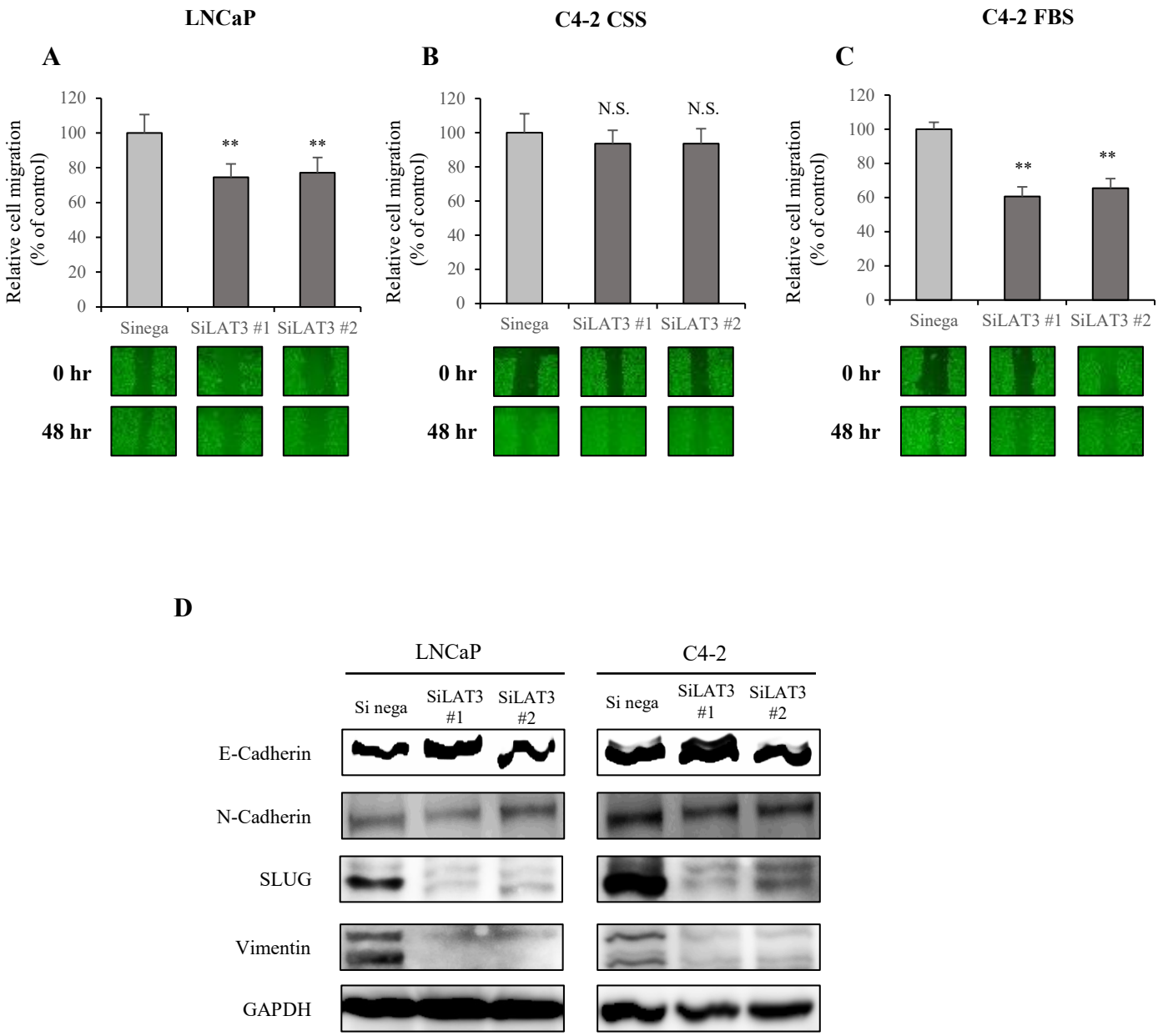

Figure S7. Effects of SiLAT3 on the wound healing and the expression of EMT-related proteins in PC cells. (A to C) SiLAT3 significantly reduced the wound healing in LNCaP cells (A) and C4-2 cells in FBS (C), but not C4-2 cells in CSS (B). (D) Effect of SiLAT3 on the expression of EMT-related proteins in LNCaP and C4-2 cells. GAPDH was used as a loading control.

Figure S8

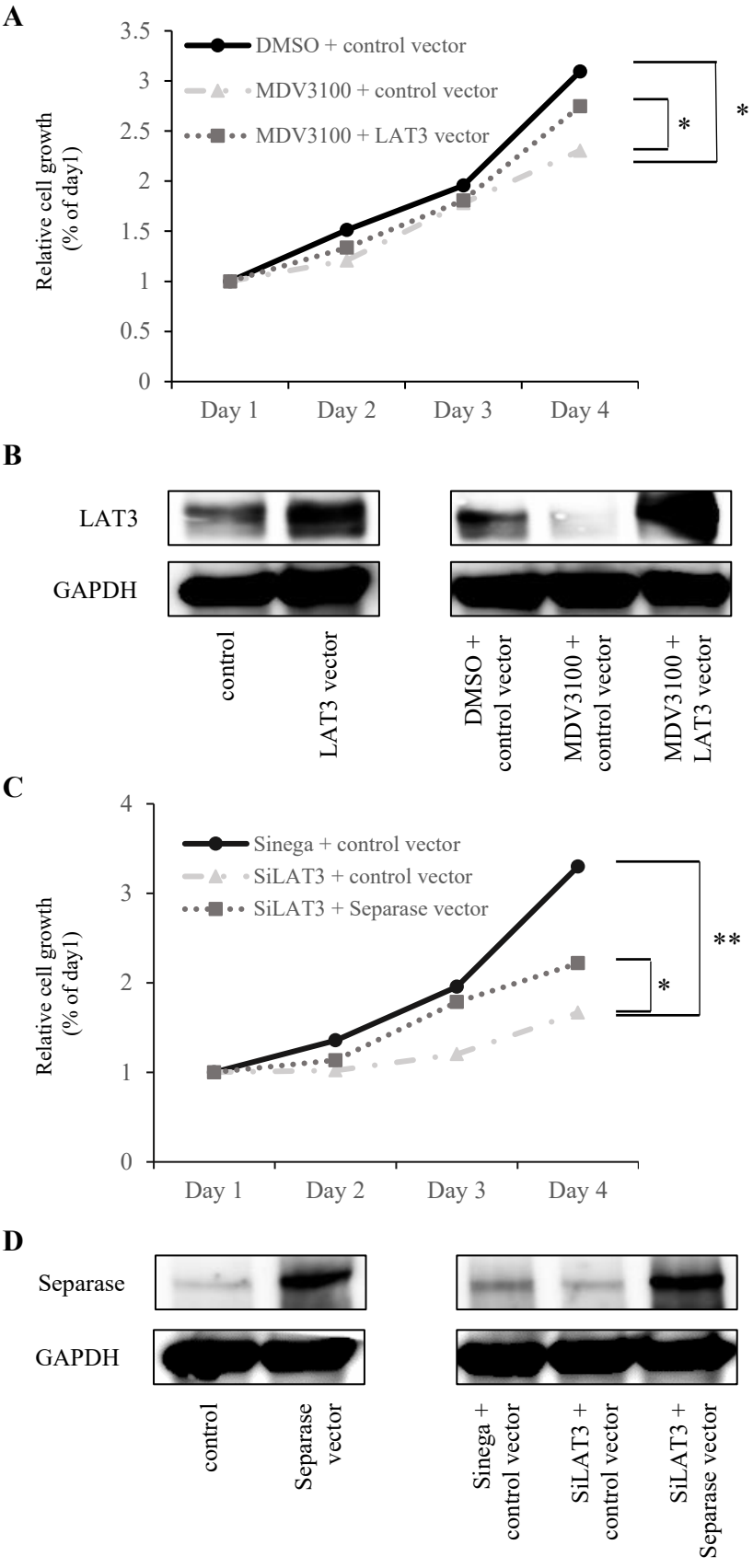

Figure S8. Knock down and rescue effect of LAT3 or Separase on cell proliferation.
(A) Knock down and rescue effect o LAT3 vector on cell proliferation. (B) Effect of MDV3100 and LAT3 vector on the expression of LAT3 in LNCaP cells. GAPDH was used as a loading control. (C) Knock down and rescue effect of Separase vector on cell proliferation. (D) Effect of SiLAT3 and Separase vector on the expression of LAT3 in LNCaP cells. GAPDH was used as a loading control. Sinega: siRNA negative control, *P < 0.05, **P < 0.01.

Figure S9

A

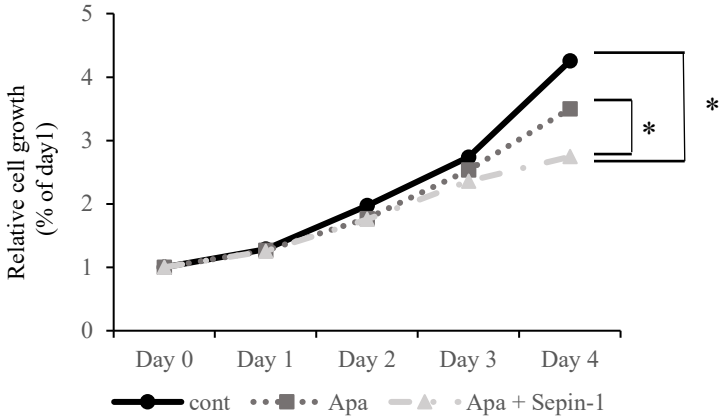

B

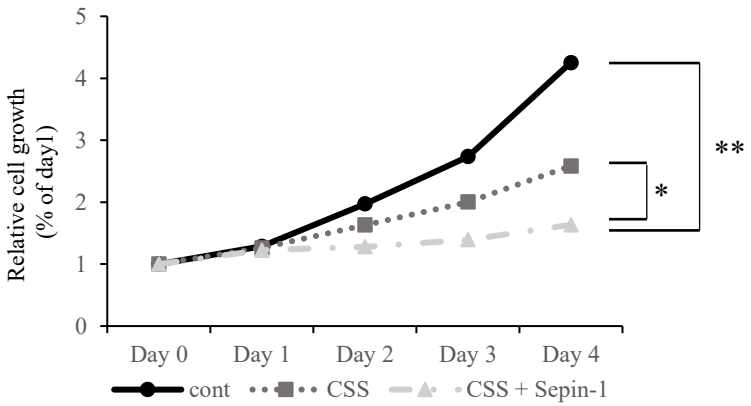

Figure S9. Validation of the additive effect of Separase inhibitor and AR inhibitor on LNCaP cell proliferation.

(A) Additive effect of Sepin-1 on apautamide. (B) Additive effect of Sepin-1 on CSS medium.
(B) *P < 0.05, **P < 0.01 (unpaired Student's t-test).

Figure S10

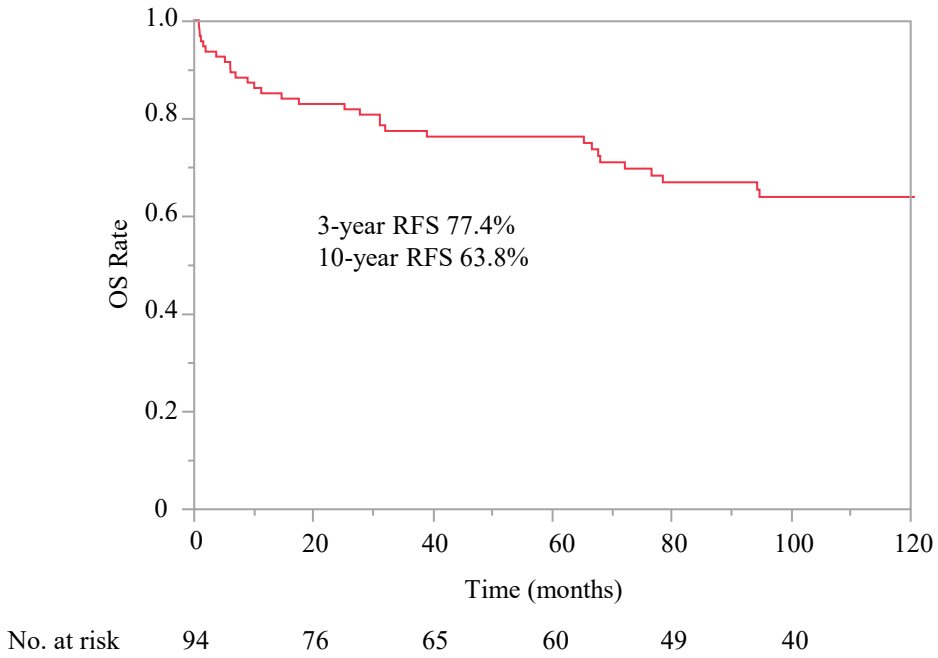

Figure S10. Kaplan-Meier analysis of RFS in all patients.

Figure S11

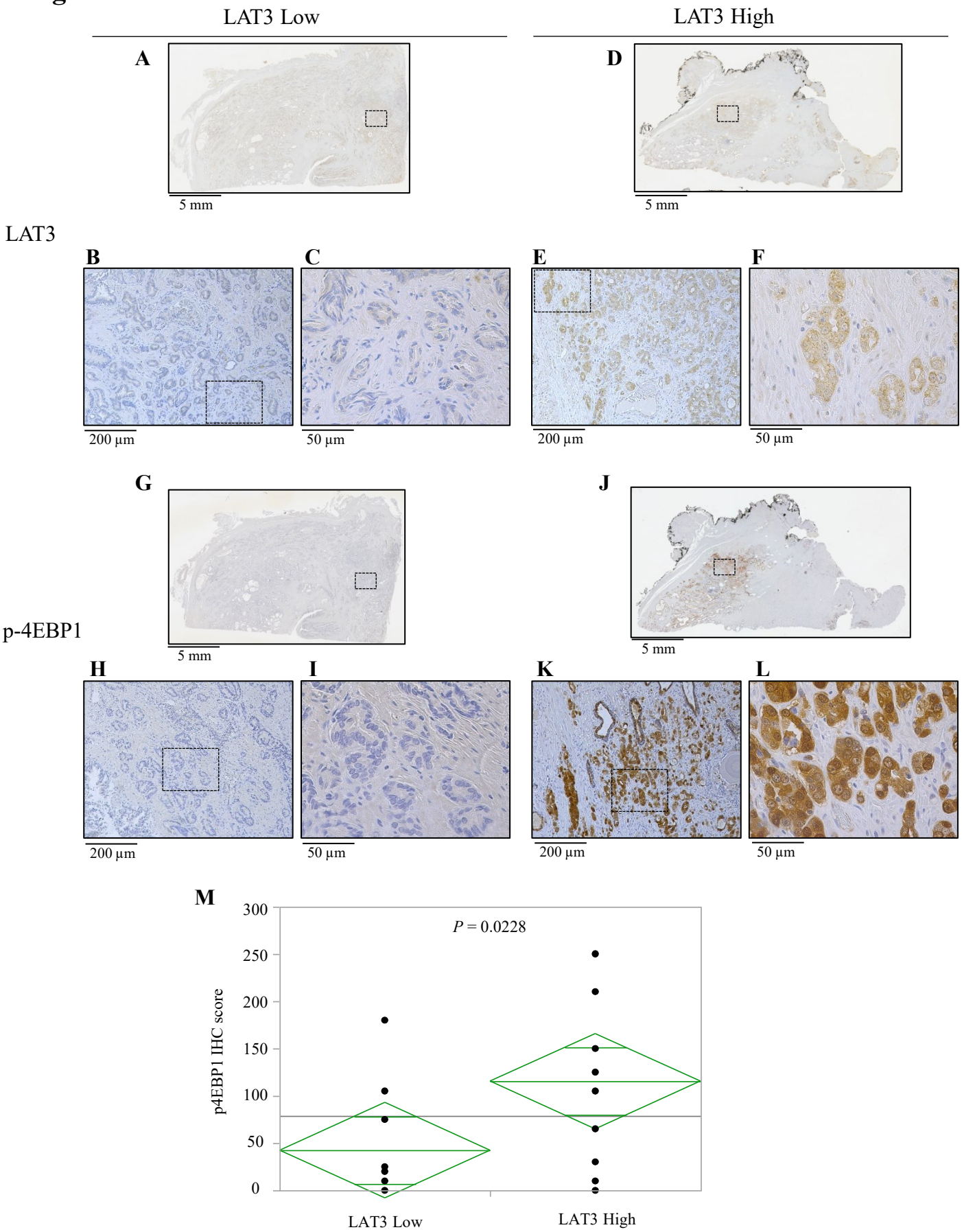

Figure S11. Immunostaining for LAT3 and p-4EBP1 in prostatectomy specimens, and their relationship. (A-L) Representative images of LAT3 immunostaining of patient in LAT3 Low group (A to C) and High group (D to F), and of p-4EBP1 immunostaining of patient in LAT3 Low group (G to I) and High group (J to L). (M) Comparison of p-4EBP1 IHC score of LAT3 Low and High group.

Figure S12

A

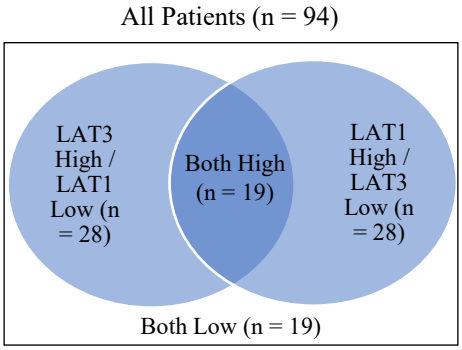

B

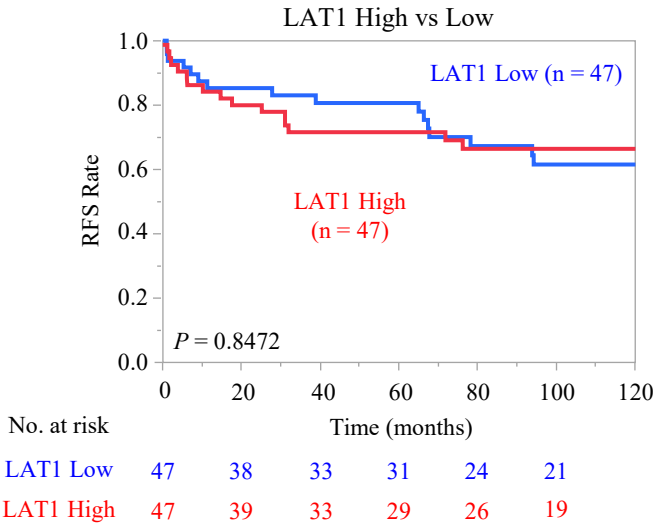

Figure S12. Relationship of IHC score between LAT3 and LAT1.
(A) Venn diagram of the distribution of the number of patients with high and/or low LAT3 and LAT1 scores.
(B) (B) Kaplan-Meier analysis of RFS according to high or low LAT3 scores.
The P value was calculated by the log-rank test.

Table 1. Univariate and multivariate Cox proportional hazard models for RFS.

Variable	Univariate			Multivariate		
	HR	95% CI	*P* value	HR	95% CI	*P* value
Age (over 66), years	1.04	0.51 - 2.19	0.9234			
Initial PSA (over 7.825), ng/mL	1.44	0.71 - 3.01	0.3102			
BMI (over 13.7)	1.07	0.52 - 2.37	0.4316			
TST (over 4.3), ng/dL	1.24	0.60 - 2.52	0.2530			
pT stage (3 or 4)	7.04	3.26 - 16.9	< 0.0001	4.10	1.72 - 10.8	0.0011
GG (4 or 5)	2.07	0.99 - 4.19	0.0529			
LAT3 score	3.24	1.53 - 7.46	0.0018	2.46	1.13 - 5.80	0.0234
Separase score	1.96	0.96 - 4.25	0.0656			
RM	4.44	2.01 - 11.2	< 0.0001	1.69	0.65 - 4.83	0.2907
ly	1.94	0.46 - 5.54	0.3183			
v	6.46	1.52 - 18.8	0.0159	3.83	0.84 - 12.8	0.0769
pn	2.93	1.28 - 7.89	0.0093	1.57	0.616 - 4.59	0.3588

RFS = reccurence-free survival; HR = hazard ratio; CI = confidence interval; PSA = prostate-specific antigen; GG = grade group; BMI = body mass index; TST = testosterone; RM = resection margin; ly = lymphatic invasion; v = vascular invasion; pn = perineural invasion

Table 2. Patient background.

Characteristics	
No. patients	94
Median age at diagnosis (range), years	66 (50 - 75)
Median initial PSA (range), ng/mL	7.825 (0.62 - 39.06)
Median BMI (range)	23.6 (16.6 - 29.87)
Median TST (range), ng/dL	4.86 (0.42 - 10.98)
Pathological T stage, n (%)	
T2	58 (61.70)
T3	35 (37.23)
T4	1 (1.07)
ISUP grade, n (%)	
1	13 (13.83)
2	28 (29.79)
3	26 (27.66)
4	9 (9.57)
5	18 (19.15)
RM, n (%)	47 (50)
ly, n (%)	7 (7.45)
v, n (%)	3 (3.19)
pn, n (%)	59 (62.77)
No. recurrence, n (%)	31 (32.98)
RFS rate	3-year: 77.4% 10-year: 63.8%

RFS = reccurence free survival; HR = hazard ratio; CI = confidence interval; PSA = prostate-specific antigen; BMI = body mass index; TST = testosterone; RM = resection margin; ly = lymphatic invasion; v = vascular invasion; pn = perineural invasion; ISUP = International Society of Urological Pathology

Supplementary Table 1. Primer sequences for RT-PCR.

Gene	Primer types	Sequence (5' to 3')
LAT3 (SLC43A1)	Forward	CCCCAACTCAGGGCACTGT
	Reverse	GTAGCGTGGTCTGATGGATTTG
AR	Forward	CCTGGCTTCCGCAACTTACAC
	Reverse	GGACTTGTGCATGCGGTACTCA
Separase *(ESPL1)*	Forward	CTGAGCCTAAAGACGGATGC
	Reverse	CTGAGTCTTCCCCGTCAGAG
PGC	Forward	TTCCCTCTGCCACCTTCCT
	Reverse	CGACTCCCACGGTGCAGTA
ESCO2	Forward	TAATGAATTGGGCTTCCAGC
	Reverse	AGGGGTGTTGCAGTACTTGG
LNPEP	Forward	TTCACCAATGATCGGCTTCAG
	Reverse	CTCCATCTCATGCTCACCAAG
LAMA1	Forward	GTTTCGAACCTCCTCGCAGA
	Reverse	CTTGCCGTCCACAAGCTCTAGT
GAPDH	Forward	CCACCCATGGCAAATTCC
	Reverse	TGATGGGATTTCCATTGATGAC

Supplementary Table 2. Characteristics of low and high LAT3 groups.

Characteristics	Low LAT3 (n = 47)	High LAT3 (n = 47)	*P* value
Median age (range), years	66 (50 - 75)	66 (52 - 75)	0.5406
Median initial PSA (range), ng/mL	7.55 (0.62 - 39.06)	7.88 (3.78 - 28.55)	0.9494
Median BMI (range)	23.3 (18.3 - 29.87)	23.8 (16.6 - 27.3)	0.2881
Median TST (range), ng/dL	5.42 (0.42 - 8.84)	4.51 (2.18 - 10.98)	0.8803
pT stage (3 or 4), n (%)	12 (25.53)	24 (51.06)	0.0190
GG, n (%)			0.0053
1, 2, 3	39 (82.98)	28 (59.57)	
4	4 (0.085)	5 (10.64)	
5	4 (0.085)	14 (29.79)	
RM, n (%)	20 (42.55)	27 (57.45)	0.2156
ly, n (%)	4 (8.51)	3 (6.38)	0.7826
v, n (%)	1 (2.13)	2 (4.26)	0.8790
pn, n (%)	29 (61.70)	30 (63.83)	0.6650

PSA = prostate-specific antigen; GG = grade group; BMI = body mass index; TST = testosterone; RM = resection margin; ly = lymphatic invasion; v = vascular invasion; pn = perineural invasion

Supplementary Table 3. Characteristics of low and high Separase groups.

Characteristics	Low Separase (n = 46)	High Separase (n = 48)	*P* value
Median age (range), years	66 (50 - 75)	65.5 (54 - 75)	0.5888
Median initial PSA (range), ng/mL	7.525 (2.45 - 39.06)	7.875 (0.62 - 28.55)	0.6829
Median BMI (range)	23.3 (16.6 - 27.67)	23.9 (18.2 - 29.87)	0.3970
Median TST (range), ng/dL	5.28 (0.42 - 8.84)	4.64 (2.18 - 10.98)	0.5827
pT stage (3 or 4), n (%)	13 (38.26)	23 (47.92)	0.0587
GG, n (%)			< 0.0001
1, 2, 3	42 (91.30)	25 (52.08)	
4	4 (0.087)	5 (10.41)	
5	0	18 (37.5)	
RM, n (%)	20 (43.48)	27 (56.25)	0.3022
ly, n (%)	3 (6.52)	4 (8.33)	0.7645
v, n (%)	1 (2.17)	2 (4.17)	0.8710
pn, n (%)	27 (58.70)	32 (66.67)	0.5229

PSA = prostate-specific antigen; GG = grade group; BMI = body mass index; TST = testosterone; RM = resection margin; ly = lymphatic invasion; v = vascular invasion; pn = perineural invasion

雑誌名：Cancer Science
巻・号：　第　　112　巻　　第　　9　　号
頁：　　3871 頁　～　　3883 頁掲載
2021年5月29日　公表済み
DOI: 10.1111/cas.14991